HYDRATES IN NATURAL GAS TRANSPORT – PROBLEMS AND REMEDIES

A Project Report submitted in partial fulfillment of the requirements for
the Degree of
MASTER OF TECHNOLOGY
in
GAS ENGINEERING
(Academic Session 2003-05)

By
L.ANANTH

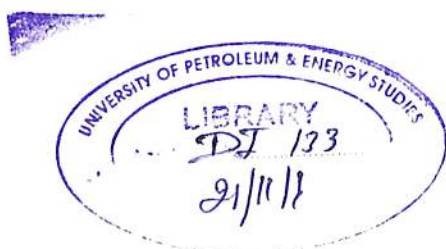Under the Supervision of

Dr. B.P. PANDEY

COLLEGE OF ENGINEERING STUDIES
UNIVERSITY OF PETROLEUM & ENERGY STUDIES
DEHRADUN (U.A) 248007
May 2005

HYDRATES IN NATURAL GAS TRANSPORT
– PROBLEMS AND REMEDIES

A Project Report submitted in partial fulfillment of the requirements for
the Degree of
MASTER OF TECHNOLOGY
in
GAS ENGINEERING
(Academic Session 2003-05)

By
L.ANANTH

Under the Supervision of

Dr. B.P. PANDEY

COLLEGE OF ENGINEERING STUDIES
UNIVERSITY OF PETROLEUM & ENERGY STUDIES
DEHRADUN (U.A) 248007
May 2005

CERTIFICATE

This is to certify that the Project Report on *"Hydrates in Natural Gas Transport-Problems And Remedies"* submitted to University of Petroleum & Energy Studies, Dehradun, by **Mr. L.Ananth,** in partial fulfillment of the requirement for the award of Degree of Master of Technology in Gas Engineering (Academic Session 2003-05) is a bonafide work carried out by him under my supervision and guidance. This work has not been submitted anywhere else for any other degree or diploma.

Date: May 24,05

Dr.B.P.Pandey

TABLE OF CONTENTS

Executive Summary

Unrestricted fluid flow of oil and gas streams is crucial to the petroleum industry. Unless preventative action is taken, gas hydrate plugs form under the high pressure, low temperature conditions inherent to offshore production.

The oil and gas industry is facing increasing costs in inhibiting gas hydrate formation due to the development of offshore gas reservoirs. Recent international estimates of the cost of the conventional inhibitor, methanol, alone are in excess of $150 million/year. Gas hydrates are likely to form in sub sea flow lines unless the water is removed down to the lowest dew point encountered, highly effective insulation is in place, or inhibitors are used. Since complete stripping of water from condensates and/or natural gas is prohibitively expensive, and effective insulation is beyond current economic limits, the most effective solution includes the use of hydrate inhibitors.

This project describes the state of the art of hydrate prevention, detailing hydrate structure, conditions and mechanisms of formation, and developing approaches - from the conventional to the cutting-edge - to hydrate inhibition. Its focus on low-dosage inhibitors, including a review of kinetic inhibitors and anti-agglomerants form, function, development, selection and applications, highlights gaps in current knowledge. Finally, a research agenda addressing both mitigation and deployment strategies is proposed.

CHAPTER-1
INTRODUCTION

1 Introduction

Hydrate formation is a substantial problem in deepwater production and underwater pipelines, which transport condensed phase hydrocarbons such as gas condensate or crude oil. In these situations, once plugs have formed, there are limited possibilities for removal. In the presence of water, and under a fixed range of pressure and temperature conditions, specific to each hydrocarbon mixture, hydrates of the light gases can form. Gas hydrates, which have a crystalline structure analogous to that of ice, form solid plugs and block the flow. Clearly, inhibition of hydrate formation is of utmost interest to industry.

1.1 Background

There are many transportation options for natural gas - compressed natural gas (CNG), liquefied natural gas (LNG), pipelines, and gas-to-liquid (GTL) product transportation. Pipelines are generally attractive for short distance from the shore due to the low capital investments. However pipeline transportation requires extensive gas processing which will drive the production costs up, making pipeline transportation unfeasible for low production rates and high moisture containing gases.

LNG transportation requires a very high capital investment and for this reason, should not be considered for the Hydrate Ridge site. Alternatively, CNG provides lower operating costs, but incurs high capital costs due to the transportation vessel. This makes CNG ideal for mid-sized reserves which can produce a large quantity of gas over the reserve lifetime to absorb the capital cost of vessel. CNG is an attractive alternative if natural gas hydrate and GTL transportation proves to be a technical challenge or the production costs become too high. GTL transportation has the lowest capital investment

for the processing equipment to produce the liquids, but GTL transportation is uneconomical at this point. If the economics of syn-gas production is lowered, GTL transportation is very attractive and should be considered as the mode of transportation.

Figure 1.1 illustrates the relationship of annual production rate and distance from the market to the modes of gas transportation. As illustrated, LNG is not a feasible option for short distances or low production rates. The figure presents GTL transportation as feasible for long distances for low production rates, this is because of the high capital cost for the GTL processors and CNG and NGH become more economically feasible at shorter distances. However, this can be argued and CNG for Hydrate Ridge sites is not as economically viable as hydrate shipping. The estimates for the economics used by Gudmundsson assume poor GTL conversions based on previous technologies. GTL technologies are becoming more economical and efficient and should not be ignored. Based on this analysis hydrates, GTL and CNG are the more economical transportation modes with CNG being a fall back if hydrates prove too technically challenging and GTL processes are too costly.
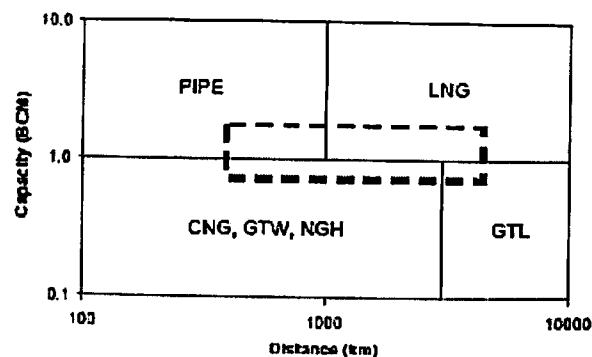

Figure 1.1 Relationship of the economics of yearly production rate and distance to the market [Gudmundsson, 2003].

Source: A generalized solubility-supersolubility diagram after Mullin(1993).

Since the 1930's when Hammerschmidt determined that the material plugging pipelines were gas hydrates, interest in gas hydrates has continued to increase. Hammerschmidt's discovery led to the regulation of the water content in natural gas pipelines. In 1934, Hammerschmidt published a correlation summary of over one hundred hydrate formation data points.

1.2 Scope of Work

Unrestricted and problem-free flow of petroleum products during extraction, processing and transportation is essential to the oil and gas industry. Whether heavy hydrocarbons such as crude oil, or low molecular weight hydrocarbons such as natural gas and natural gas liquids are the target end product, natural gas is almost always present in the fluid extracted during production. To varying degrees (most often low early in the life of a reservoir and high toward the end), the extracted oil and gas mixture also contains water. In the presence of water, and under a fixed range of pressure and temperature conditions, specific to each hydrocarbon mixture, hydrates of the light gases can form. Gas hydrates, which have a crystalline structure analogous to that of ice, form solid plugs and block the flow. Clearly, inhibition of hydrate formation is of utmost interest to industry.

Hydrate formation is a substantial problem in deepwater production and underwater pipelines, which transport condensed phase hydrocarbons such as gas condensate or crude oil. In these situations, once plugs have formed, there are limited possibilities for removal.

Since the 1970's, the oil and gas industry has faced increasing costs associated with inhibition of gas hydrate formation, due to the development of offshore gas reservoirs. Recent international estimates of the cost of the conventional inhibitor, methanol, alone, are in excess of $150 million/year. Gas hydrates are likely to form in

sub sea flow lines unless the water is removed down to the lowest dew point encountered, highly effective insulation is in place, or inhibitors are used. The first option is difficult when supersaturated condensates exist in the flow line even after the gas phase is stripped to saturation levels. Stripping condensate completely of water is prohibitively expensive and effective insulation is beyond current economic limits. Therefore, the most effective solution appears to be the use of inhibitors. Generically, there are two kinds of hydrate inhibitors: thermodynamic inhibitors, and the more recently identified low-dosage inhibitors. Thermodynamic inhibitors have been in use for a long time, and continue to be the industry standard. This kind of inhibitor works as an antifreeze by involving the water in a thermodynamically favourable relationship, so that it is not available for reaction with the gas.

It is only in recent years that low-dosage inhibitors have been sufficiently developed to justify application in the field. Because they constitute one of the newest approaches to resolving the hydrate formation problem, they remain the least studied (both in the lab and in the field), the most poorly understood and modeled, and the least applied, although applications in some field conditions are recorded. For the same reasons, low-dosage inhibitors hold the greatest promise for breakthrough solutions to hydrate inhibition in the next few years.

Recently, low-dosage inhibitors have been introduced in industry. Even though they are more expensive than conventional inhibitors (methanol and glycol) on a per unit basis, they have gained popularity because only small quantities are required to inhibit hydrate formation. In addition to the savings in operating costs, implementation of low-dosage inhibitors is expected to reduce environmental costs and capital expenditures. Methanol is toxic, and both methanol and glycol must be removed from hydrocarbon stream before going to the market (a regeneration system is required). Low-dosage inhibitors, on the other hand, do not need to be removed from the product stream; capital

2005

and operating costs associated with separation and recycling systems required when other families of chemical inhibitors are used, are thereby eliminated. Low-dosage inhibitors are usually non-toxic and/or biodegradable substances, which provide an environmental friendly technology. However, some of these chemicals have not been approved in certain jurisdictions. Considerations of regional environmental regulations should be taken when selecting and deploying this new technology.

1.3 Organization of Project

This project begins by describing the conditions and mechanisms of hydrate formation and relates them to the approaches to hydrate inhibition currently used in industry. Limitations of each are described. It is the goal of this project to examine the state-of-the-art in the understanding and application of low-dosage inhibitors for the purpose of formulating a research agenda which will help realize the potential of these inhibitors as a solution to the critical problem of hydrate formation in oil and gas production.

2 Gas Hydrates Description

A gas hydrate is a crystalline solid that forms under the specific conditions of temperature and pressure, which are thermodynamically appropriate to that gas. "Hydrate" refers to the fact that water molecules surrounding a central molecule of a different kind form them. In the case of gas hydrates, this central molecule is a low molecular weight gas, such as those, which commonly constitute natural gas; i.e., methane, ethane, propane, and iso-butane, SO_2, N_2, H_2S, CO_2, and others – more than one hundred formers have been identified. The water molecules form a repetitive geometric lattice, which is commonly referred to as a cage. Without the gas molecule at the center, the highly organized cage structure would be in dynamic equilibrium with free flowing water molecules, perpetually forming and collapsing. In the presence of the central gas molecule, given the right conditions of temperature and pressure, the water molecule-based cage forms a geometric structure (usually having twelve, fourteen, or sixteen sides). This structure is stabilized by the additional Vander Waals forces acting between the gas molecule and the surrounding water molecules. On the range of a few Angstroms, solid nuclei form, and begin to grow. When nuclei come in contact with other nuclei and join together to form larger particles, the process is called agglomeration. Attraction between neighbouring apolar molecules inside the cages of water molecules causes the agglomeration. Once the growing structure achieves a critical minimum size (8-30 nm), rapid growth of hydrate crystals, known as catastrophic growth ensues. Hydrate crystal nucleation and growth is a kinetic process, meaning that hydrates do not appear instantaneously with the onset of thermodynamically favourable conditions. The lag between the time when system conditions favour hydrate formation and the appearance of hydrates is known as induction time.

CHAPTER-2
GAS HYDRATE DESCRIPTION

2.1 Review of Gas Hydrate Formation

Researchers have usually studied the hydrate formation process to better understand the performance of kinetic inhibitors. However more recently, hydrate formation has been in focus in the production of hydrates for storage and transport of natural gas, gas separation, exploitation of gas hydrate deposits and depositing of CO_2 hydrates on the sea floor. The increasing number of published articles on hydrate formation in the four consecutive international gas hydrate conferences (Sloan, Happel and Hnatow, 1994, Monfort, 1996, Holder and Bishnoi, 2000, Mori, 2002) illustrates the large interest in hydrate formation issues.

This chapter is intended to give a review of hydrate formation studies with emphasis on the rate of gas hydrate formation in water continuous systems under stirred conditions. With some exceptions, the review is limited to systems where the hydrate forming components are hydrocarbons. The macroscopic studies of hydrate formation, which are most relevant to the present work, are stressed.

2.2 Hydrate Structures

Gas hydrates are crystalline solids. They are more properly called clathrate hydrates to distinguish them from stoichiometric hydrates found in inorganic chemistry. The crystalline structure is composed of polyhedra of hydrogen bonded water molecules. The polyhedra form cages that contain at most one guest molecule each. The cages are stabilized by vander Waals forces between the water molecules and the enclatherated guest molecule. In extraordinary situations, two guest molecules may enter the same cage (Sloan, 1998).

Only a few kinds of cages may form depending on the size of the guest molecule. These cages arrange into different hydrate structures known as structure I (sI), structure II (sII) and structure H (sH) (Sloan, 1998). Recently, Udachin and Ripmeester (1999) discovered a new and complex hydrate structure consisting of alternating stacks of sH and sII. Methane gas forms sI hydrates, while natural gas usually forms sII hydrates. sI and sII hydrates will be discussed further.
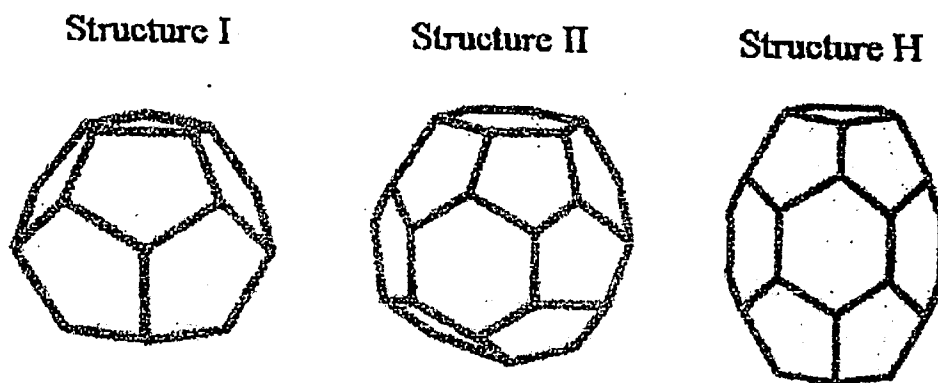
Structure I   **Structure II**   **Structure H**

Figure 2.1 Schematics of structure I, II & H gas hydrates

Source: A generalized solubility-supersolubility diagram after Mullin(1993).

sI consists of two different cages. In a unit cell, 2 small and 6 large cages appear. The small cage, the pentagonal dodecahedron labeled 5^{12}, has 12 pentagonal faces with equal edge lengths and equal angles. The large cage, the tetrakaidecahedron, is called $5^{12}6^2$ because it has 12 pentagonal and 2 hexagonal faces. One sI unit cell has 46 water molecules and fits into a 12 Å cube. sII consists of 16 small cages and 8 large cages. Also, sII has the pentagonal dodecahedron (5^{12}) as the small cage. The large cage, the

hexakaidecahedron, has 12 pentagonal and 4 hexagonal faces and is therefore labeled $5^{12}6^4$. One sII unit cell has 136 water molecules and fits into a 17.3 Å cube (Sloan, 1998).

Only a few kinds of cages may form depending on the size of the guest molecule. These cages arrange into different hydrate structures known as structure I (sI), structure II (sII) and structure H (sH) (Sloan, 1998). Recently, Udachin and Ripmeester (1999) discovered a new and complex hydrate structure consisting of alternating stacks of sH and sII. Methane gas forms sI hydrates, while natural gas usually forms sII hydrates.

sI consists of two different cages. In a unit cell, 2 small and 6 large cages appear. The small cage, the pentagonal dodecahedron labeled 5^{12}, has 12 pentagonal faces with equal edge lengths and equal angles. The large cage, the tetrakaidecahedron, is called $5^{12}6^2$ because it has 12 pentagonal and 2 hexagonal faces. One sI unit cell has 46 water molecules and fits into a 12 Å cube. sII consists of 16 small cages and 8 large cages. Also, sII has the pentagonal dodecahedron (5^{12}) as the small cage. The large cage, the hexakaidecahedron, has 12 pentagonal and 4 hexagonal faces and is therefore labeled $5^{12}6^4$. One sII unit cell has 136 water molecules and fits into a 17.3 Å cube (Sloan, 1998).

Generally, molecules between 3.8 Å and 6.5 Å in diameter can form sI and sII hydrates if they do not contain hydrogen bonding group(s). Depending on the size of the guest molecules, only the large cages of each structure can be occupied or both types of cages can be occupied. The small cages are never occupied alone as this is not enough to stabilize either sI or sII. However, if the small cages can be filled, the molecule will also enter the large cages as a simple hydrate species. Simple hydrates are hydrates with only one guest species (Sloan, 1998).

The large cages in sI ($5^{12}6^2$) are large enough to contain molecules up to 6.0 Å in diameter, in which only ethane and carbon dioxide of the natural gas components

stabilize as simple hydrates. The large cages in sII can contain molecules as large as 6.6 Å. This means that propane and iso-butane will stabilize the large cages, but leave the small cages of sII vacant. Alternatively, the small cages are filled with methane, which means that natural gas with propane or iso-butane typically forms sII hydrates. Methane will form sI hydrate by filling both the large and the small cages, but not sII because the molecules are too small to stabilize the large cages in sII.

Based on the knowledge about the hydrate structure for a given gas composition, it is possible to calculate the relative water/guest ratio known as the ideal hydration number. Pure methane will occupy the 2 small and the 6 large cages of sI. With 46 water molecules in a unit cell, the ideal hydration number becomes 5.75. For an natural gas mixture of methane, ethane and propane, where propane and ethane stabilize the 8 large cages of sII, methane enter the 16 small cages, and the unit cell has 136 water molecules, the ideal hydration number becomes 5.67.
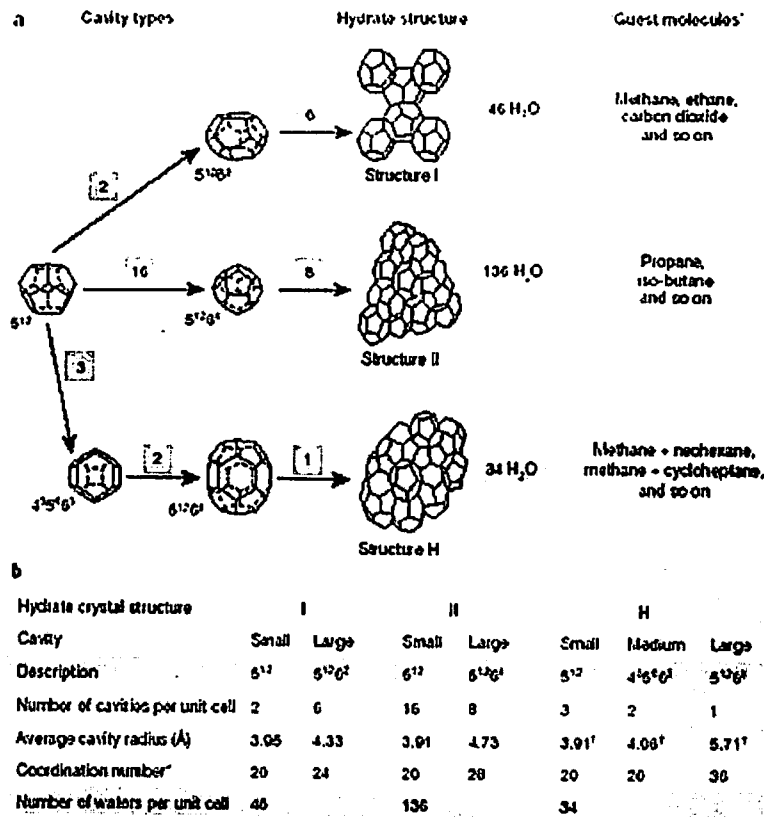
Figure 2.2 *Three common hydrate unit crystal structures*

Source: *A generalized solubility-supersolubility diagram after Mullin(1993).*

If all the cages of sII had been filled, each volume of hydrate would have contained 182 standard volumes of gas (1 atm, 15 °C). In reality however, it is impossible to obtain a perfect crystal where all the cages are filled, which means that the real hydration number is higher than the ideal hydration number. The degree of filling depends on the system conditions. This variation in filling degree demonstrates why hydrates are non-stoichiometric clathrate compounds.

2.3 Hydrate Equilibrium Conditions

At hydrate equilibrium conditions, solid hydrate may exist in equilibrium with liquid water or ice, gas and some additive. Such temperature and pressure conditions are defined by the hydrate equilibrium curve for a given gas and water composition. Hydrates can only form at temperatures lower than the equilibrium temperature and simultaneously at pressures higher than the equilibrium pressure. The distance from the equilibrium conditions is the driving force for hydrate formation. Hence, the hydrate equilibrium curve represents the pressure and temperature conditions where the hydrates dissociate. The hydrate equilibrium curves for methane and a natural gas mixture (92 % methane, 5 % ethane and 3 % propane) are shown in figure 2.3.
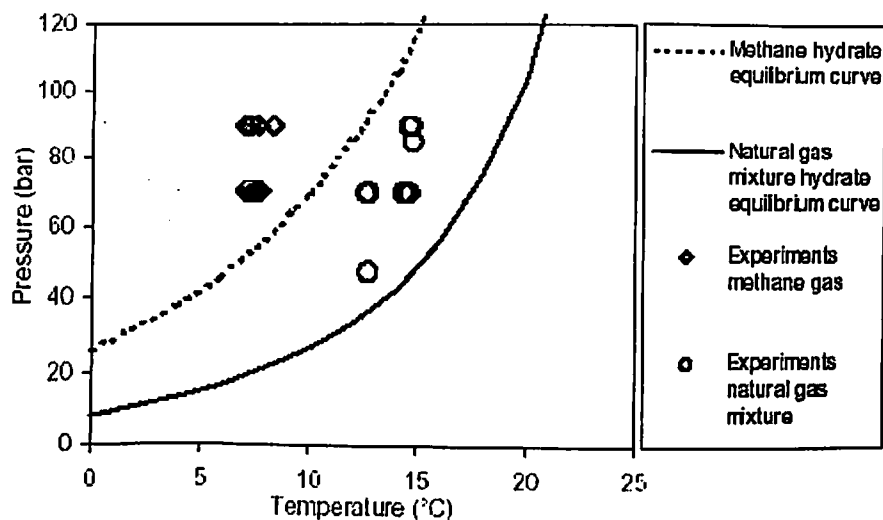

Figure 2.3 Hydrate equilibrium curves for methane gas and natural gas mixture
Source: A generalized solubility-supersolubility diagram after Mullin(1993).

Hydrate equilibrium curves can be predicted from statistical thermodynamics using the vander Waals and Platteeuw model with some modifications, which is

thoroughly explained by Sloan (1998). Also, other simpler methods based on hand calculation and phase diagrams exist (Sloan, 1998). Available computer programs based on statistical thermodynamic models, such as CSMhyd (1998) or PVTsim (2001) can predict hydrate equilibrium conditions.

The hydrate equilibrium temperature at 1 atm is -73 °C for methane gas and -36 °C for natural gas mixture (PVTsim, 2001). At these temperatures, hydrates are thermodynamically stable. On the other hand, Gudmundsson, Parlaktuna and Khokhar (1992) observed that the natural gas concentration in hydrate samples remained almost unchanged when stored at atmospheric pressure and at -18 °C for periods of 10 days. This behavior was explained by the formation of an ice layer around the hydrate crystals.

2.4 Mechanisms of Gas Hydrate Formation

The thermodynamic behavior of hydrate systems forms the basis for understanding the mechanisms of hydrate formation. The time-dependent phenomenon of hydrate formation kinetics is described by applying crystallization theories including nucleation, growth, agglomeration and breakage. So far, the most studied phenomena of gas hydrate formation are the nucleation and growth processes.

Nucleation is a microscopic stochastic phenomenon where gas-water clusters (nuclei) grow and disperse until some nuclei have grown to a critical size. Nucleation may occur spontaneously (homogeneous nucleation), or it may be induced around impurities (heterogeneous nucleation). In contrast to primary nucleation, where nucleation commences without crystals present, secondary nucleation occurs in the vicinity of already growing crystals in the system.

The time from the first gas-liquid contact to the first detection of a hydrate phase is called the induction time. In macroscopic studies, the induction time has been used as a

measure of the nucleation period (Skovborg *et al.,* 1993, Monfort and Nzihou, 1993, Yousif, 1994, Natarajan, Bishnoi and Kalogerakis, 1994). These studies indicate that the induction time increases dramatically when the driving force for hydrate formation approaches zero.

In 1991, Sloan and Fleyfel presented a molecular mechanism for gas hydrate nucleation from ice. The mechanism is based on observations of methane and krypton hydrate formation from ice, where induction times were clearly observed, and ethane hydrate formation, where no induction time was observed. Sloan and Fleyfel suggested that on an ice surface, free water molecules rearrange around a guest molecule to form an unstable 512 cage. Methane and krypton molecules, which enter this cage, oscillate between the 512 cages of sI and sII before the cages reach a stable nuclei size. Ethane does not experience the induction time because ethane stabilizes the large cages of sI, and hence, ethane does not induce oscillation between the small cages. Yousif (1994) argued that hydrate formation always starts by stabilizing the large cages of sI and sII regardless of the size of the guest molecule.

Christiansen and Sloan (1994) extended the mechanism of Sloan and Fleyfel (1991) to explain hydrate formation in liquid water. They suggested four stages: molecular species, labile clusters, metastable agglomerates and stable nuclei. As gas dissolves in water, hydrogen-bonded water molecules gather around the apolar guest molecule to form labile clusters. Depending on the guest size, the number of water molecules in each cluster, defined by a coordination number, varies. Because the guest molecules inside the clusters are attracted to each other, the labile clusters agglomerate. However, two different coordination numbers of each hydrate structure are required to form agglomerates, or else the nucleation is inhibited until the clusters transform to fulfill the coordination number requirement. The agglomerates are in quasi equilibrium with

each other and other labile clusters until they exceed the critical size for stable nuclei. Stable growth begins.

In contrast to Christiansen and Sloan (1994), who assumed hydrate nucleation in the liquid water phase, Rodger (1990) developed a model based on nucleation at a surface. Rodger suggested that the hydrate forming molecules are adsorbed on a water or ice surface and condensed water molecules orient around the guest molecules to form cages. Some cages may rearrange to form liquid water and free guest molecules, others may grow to eventually form stable nuclei.

Kvamme (1994) critically reviewed the mechanisms of Christiansen and Sloan (1994) and Rodger (1990). He stated that the main difference is that Christiansen and Sloan relate nucleation to the liquid phase or at least the liquid side of the gasliquid interface, while Rodger relates it to the gas side of the gas-liquid interface. Kvamme noted that the mechanism of Christiansen and Sloan contained no element of randomness or probability. Considering the mechanism of Rodger, nonhydrate formers may adsorb on the surface and cause inhomogeneous hydrateforming properties of the surface. This introduces an element of probability that can explain observed variety of induction times in parallel experiments.

In 1996, Kvamme proposed a new hydrate formation theory based on the hypothesis that initial hydrate formation takes place at the gas-liquid interface towards the gas side (Rodger, 1990). The theory was modeled and compared to experimental data. Kvamme (2000) published a revised version of the model where evaluation of cluster distribution and cluster stability analysis are included. An extended diffusive interface theory models the growth rates of the metastable clusters. Comparison of modeled growth rates towards the gas side and towards the liquid side of the gas-liquid interface

indicates that the gas side growth rates are two orders of magnitude higher than the liquid side growth rates (Kvamme, 2002).

Mechanisms to describe growth have received less attention. Sloan (1998) considered growth to be a combination of mass transfer of components to the growing surface and growth at the hydrate surface. He suggested a hypothesis adopted from classical crystallization including adsorption of the cluster at the hydrate surface, diffusion over the surface and integration of the cluster into a kink.

2.5 Driving Forces for Gas Hydrate Formation

Mullin (1993) defines the driving force for crystallization in terms of supersaturation. Spontaneous (homogeneous) nucleation will only occur in a supersaturated solution in the labile zone limited by the supersolubility curve (Figure 2.4). In the metastable zone, spontaneous nucleation cannot occur, but growth of crystals is possible. For instance, the driving force for nucleation and growth can be defined by the supersaturation ratio: the concentration of the supersaturated solution to the equilibrium concentration at the solubility curve, both at the same temperature.
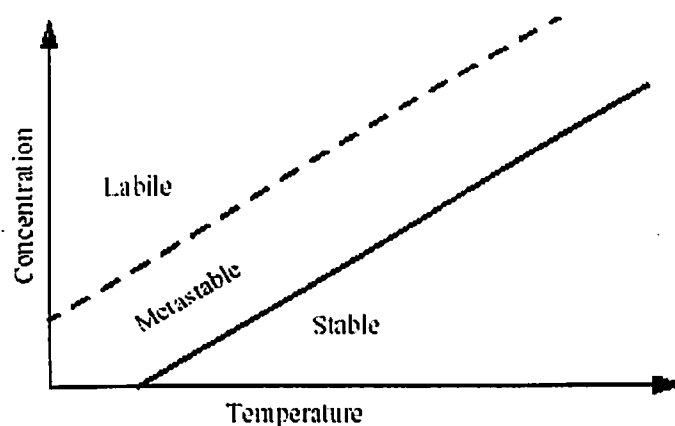
Figure 2.4 The continuous line is the solubility curve and the broken line is the
supersolubility curve.

Source: *A generalized solubility-supersolubility diagram after Mullin(1993).*

Sloan (1998) suggested an analogy to hydrate formation where concentration is replaced by the logarithmic pressure giving the hydrate equilibrium curve. A corresponding supersolubility curve has not yet been defined in hydrate kinetic studies. Several driving forces have been used in modeling of hydrate formation kinetics, and those most frequently used in experimental studies are related to the hydrate equilibrium curve.

Vysniauskas and Bishnoi (1983, 1985) used subcooling (sometimes also called supercooling) as the driving force for nucleation and growth. Subcooling is defined as the difference between the hydrate equilibrium temperature at the experimental pressure and the experimental temperature. Subcooling is easily determined by measuring the experimental temperature and calculating the hydrate equilibrium temperature using a thermodynamic model.

Alternatively, the distance from the hydrate equilibrium curve in terms of pressure or fugacity can be used. Englezos *et al.* (1987) used the difference in fugacity of the dissolved gas and the hydrate equilibrium fugacity at the experimental temperature as the driving force in their hydrate formation model. Similarly, Natarajan, Bishnoi and Kalogerakis (1994) used $f''g / f_{eq} - 1$, where $f''g$ is the gas phase fugacity, as driving force for nucleation.

Sloan (1998) pointed out that a pressure or fugacity difference as a driving force does not represent physical reality. If there is no net force working on the system, the pressure everywhere in the system must be equal. In multi-phase systems, pressure equilibrium times are orders of magnitude shorter than thermal equilibrium times. Moreover, the temperature at the hydrate surface must be higher than the experimental temperature as heat is released upon hydrate formation. Therefore, subcooling is a better driving force (Sloan, 1998).

Skovborg and Rasmussen (1994) used the difference in gas mole fraction at the gas-liquid interface and in the liquid bulk phase as the driving force. They maintain that the formation rate is controlled by gas-liquid mass transfer rather than crystal growth, and therefore, the driving force is not related to the hydrate equilibrium curve or the hydrate crystal surface. In their study of induction times, Skovborg et al. (1993) expressed the driving force as the difference in the chemical potential of water in the hydrate phase and water in the liquid phase at the experimental pressure and temperature.

Similarly, Herri et al. (1999) expressed the driving force for gas dissolution in water as the difference in the gas concentration at the gas-liquid interface and in the liquid bulk. For growth of the hydrate crystals, the driving force is the difference in bulk concentration and gas concentration in the presence of a hydrate phase.

2.6 Size of Hydrate Crystals

Englezos *et al.* (1987) developed a model for the rate of hydrate formation including the total surface area of all hydrate crystals, which is found from *in situ* measurements of the particle size distribution. Englezos *et al.* could not measure the distribution in their experiments, so they calculated the surface area based on estimates of the critical nuclei size. However, this model initiated studies on methods to measure hydrate crystal sizes.

Nerheim, Svartaas and Samuelsen (1992) used a laser light scattering technique to measure the size of nuclei in a static system during the nucleation period. They found that the critical nuclei sizes are in the range 5-30 nm, which correspond well with the calculated nuclei sizes of Engelzos *et al.* (1987).

Monfort and Nzihou (1993) measured the particle size distribution using laser light scattering during cyclopropane hydrate formation. Crystals in the range 5.6 to 564 µm could be measured. The measured size evolution with time showed that the size of small crystals rapidly increases due to crystal growth and agglomeration. Monfort *et al.* (2000) found the particle size distribution during growth of ethane and propane hydrates and calculated the growth rates. The calculated maximum growth rates for ethane and propane were 0.35 and 0.045 µm/s, respectively.

Bylov (1997) tested another laser light technique, which is able to measure larger crystals than the system of Nerheim *et al.* (1992). He found that in the first part of the experiments the mean diameter of methane, ethane and natural gas hydrate crystals grows from about 7 to 12 µm.

Herri *et al.* (1996) developed a method for determination of particle size distribution using an optical sensor for measurement of the turbidity spectrum. This

equipment was used to investigate the influence of stirring on the particle size distribution during methane hydrate formation. During the experiments the crystals had a mean diameter between 10 and 22 μm (Herri *et al.* 1999). Herri, Gruy and Cournil (1996) observed that at a low stirring rate (250 RPM), the mean diameter increases, while it is constant at an intermediate stirring rate (400 RPM) and decreases at a high stirring rate (600 RPM). The total number of crystals increases most rapidly with time at the highest stirring rates. At about 500 RPM, the total amount of crystals increases at a constant rate. They found that the gas consumption rate increases linearly with stirring rate but approaches zero at about 250 RPM. Below 250 RPM they did not observe hydrate formation because the induction time was too long.

2.7 Promoters for Hydrate Formation

Some surfactants are found to promote hydrate formation, by increasing the gas content and the formation rate. Tohidi *et al.* (1996) observed that the methane hydrate formation rate increases when liquid methylcyclohexane is added. Structure H hydrates form when adding methylcyclohexane to a methane-water system. In fact, they found that the rate depends on the amount of methylcyclohexane added, which means that the liquid can act as a promoter for hydrate formation.

Zhong and Rogers (2000) reported that by adding 284 ppm of sodium dodecylsulfate to dissolve in the water phase, the rate of ethane hydrate formation is about 700 times higher than the rate for ethane hydrate formation in pure water. Similar behaviour was observed using natural gas. In addition, they noticed that interstitial water continues to convert to hydrate after agglomeration. Rogers, Kothapalli and Lee (2002) found that biosurfactants increase the natural gas hydrate formation rates in porous media up to 16 times.

Karaaslan and Parlaktuna (2000) studied the influence of three commercial surfactants on the natural gas consumption rate, and found that an anionic surfactant promotes hydrate formation at concentrations between 0.005 and 1 wt %. Compared to the initial rate of hydrate formation with pure water, the initial rate with 0.01 wt % of the anionic surfactant is about threefold.

Irvin *et al.* (2000) suggested using water-in-oil microemulsions to create a very large gas-liquid interfacial area. Such microemulsions are stabilized by a surfactant. They used the anionic surfactant bis (2-etyl) sodium sulfosuccinate and observed a very rapid ethylene hydrate formation rate in the presence of the surfactant. The use of microemulsions to promote hydrate formation presupposes that a liquid hydrocarbon is available.

CHAPTER-3
HYDRATE FORMATION

3 Hydrate Formation

Natural gases commonly transported in industry are believed to form only sII hydrates. In this work, an actual industrial natural gas was shown to form sII hydrates at low pressure, but sI hydrate at high pressure. Hydrate point data were collected using Raman' spectroscopy to determine the structure of the hydrate at the hydrate stability boundary. Measurements were carried out for a system PNG + water and PNG + water + 6 mol% sodium chloride. Quadruple points (sI-sII-Lw-V) were located for both systems at (287.7 K , 12 MPa) and (282.2 K , 22.4 MPa) respectively. Predicted pressures were found to match within 6 % error with respect to the data. However, the prediction suggests that the quadruple point should be approximately located at the same pressure. In conclusion, Raman spectroscopy can be effectively used to collect hydrate point data and structure simultaneously. Also, natural gas with a combined concentration of propane and i-butane lower than 0.5 mol% may form sI hydrates at high pressures. This emphasizes the importance of correct prediction of hydrate structure to industry.

3.1 Transition of Clathrate Hydrates

Clathrate hydrates are crystalline inclusion compounds that can form in systems containing water and at least one other compound. These solid crystals consist of a lattice of water molecules linked together by hydrogen bonds, similar to the most common water solid, ice. The lattice contains cavities of different shape and size, depending on its structure. Cavity diameters vary between 0.8 and 1.1 nm. Such structures are unstable, unless molecules of the correct size and a more or less apolar nature occupy a sufficient fraction of the cavities. The molecules occupying the cavities are called guests or hydrate formers. The lower hydrocarbons, methane through butane, are common hydrate formers, and therefore clathrate hydrates are often called gas hydrates.

The crystal structure of hydrate is either one of two cubic structures, named structure I and structure II. Diffraction data published by Jeffrey and McMullan clearly showed the peculiar microscopic structure of gas hydrates, including the position of the oxygen atoms of the water crystal lattice. Ripmeester et al. reported that hydrocarbon mixtures containing larger branched hydrocarbons form a hydrate of hexagonal structure called 'sH. Since it is difficult to determine a priori what hydrate structure is thermodynamically favored in a certain situation, the presence of certain key hydrate formers is used to assume or predict a hydrate of a certain structure.

Gas hydrates occur frequently in natural gas transportation pipelines, as water + hydrocarbon mixtures are transported at high pressure and low temperatures. In such a situation, blockage of a transport pipeline by gas hydrates is an important financial and safety risk. A crucial factor in any risk control strategy is knowledge about the thermodynamic stability boundary of hydrate phase regions. Phase boundaries are commonly predicted from hydrate phase models integrated into commercial software packages. Normally, a natural gas consists of about 85 mol% methane and smaller fractions of ethane, propane, butane and pentanes. This means that propane and i-butane are abundant enough to assure formation of sII hydrates. Thus, in pipeline situations, it is normal to assume that the most stable hydrate structure is sII.

However, transport of natural gases that are markedly different in composition will become more common. Heavy components of a natural gas are sometimes removed before transportation. There are good economic reasons for doing so, as the heavier components of a natural gas can be sold for a higher price. A side effect of this is that it will become more common to transport natural gases with a methane concentration of 97 mol% or more. Such gases, which we call processed natural gas (PNG), do not necessarily form sII hydrates, making the a priori assumption that only sII will occur in a pipeline situation invalid

There is also considerable geophysical interest in naturally occurring hydrates that may affect climate, seafloor stability, and energy recovery. Hydrate deposits exist in sea floor sediments and are formed from seawater and hydrocarbons that are either of a biogenic or thermogenic origin. Thermogenic natural gas tends to have a composition that resembles the composition of gas encountered in pipelines: about 90 mol% methane, the rest being ethane propane and higher hydrocarbons. sII is normally assumed to be the equilibrium structure of such hydrates. Biogenic gas on the other hand can contain methane up to concentrations of 99.9 mol%, leading to the assumption that the most stable hydrate structure is sI.

Ultimately, to determine the locus of the hydrate stability curve and the most stable hydrate structure for a certain system, models rely heavily on published hydrate point data for systems containing hydrocarbon hydrate formers. However, in the great majority of published hydrate equilibrium data, no independent measurement of the structure is done. Even though hydrate dissociation conditions are determined with great precision, the structure of the hydrate is assumed based on the size or chemical structure of the hydrate former.

Nonetheless, several techniques are available to measure the structure of a certain hydrate. The most important techniques are X-ray diffraction, NMR spectroscopy and Raman spectroscopy. Raman spectroscopy has already been used as a tool capable of identifying hydrate structure. Subramanian et al. performed Raman measurements on hydrates in the system water + methane + ethane. They showed that in a certain composition range the hydrate formed is of structure II, while it was commonly assumed that mixtures of methane and ethane form structure I hydrate. Since Raman spectroscopy is a non-intrusive technique, it has the advantage that it can be used to measure hydrate point data and hydrate structure simultaneously.

The need of such a technique may be apparent from the fact all of the published methane + ethane hydrate point data was reported to be sI, while it has now been shown that the hydrates measured were sII. Also, there is even uncertainty about the structure that is stable along the hydrate (H) − liquid water (Lw) − vapor (V) coexistence curve above 135 MPa in the water + methane system. Nakano et al. reported hydrate point data measured with Raman spectroscopy, i.e. using the methodology suggested and reported that they only observed sI hydrates. On the other hand, Chou et al. reported measurements with several techniques on hydrates in the methane + water system, in which they observed a new hexagonal structure that consists of the cavities normally associated with sII, hydrate (5^{12} and $5^{12}6^4$). They reported a quadruple point involving the new hydrate structure located at the hydrate stability boundary at 135 MPa. This implies that the new structure is the stable structure at the hydrate stability boundary at pressures above 135 MPa. Since this is in contradiction with what was observed by Nakano et al. even the hydrate phase behavior in the methane + water system − a well-studied system by any standard - is still unresolved. This illustrates that a tool that can complement determination of the hydrate stability boundary with structure determination is undoubtedly needed.

In this work, data have been measured up to a pressure of 70 MPa on a system consisting of water and processed natural gas (PNG). Hydrate dissociation point data have been collected using Raman spectroscopy to detect the presence of hydrate crystals and to determine what structure is present at the hydrate stability boundary. The reliability of this technique has been discussed extensively by Jager et al.

The experimental setup and the integration of Raman spectroscopy into a setup for determination of hydrate point data are discussed. The hydrate point data and evidence for a pressure induced structural transition are discussed in the experimental results section. The impact of this work is given in the concluding section.

3.2 Experimental Method

Raman spectroscopy was used as an experimental technique to measure disappearance of hydrate crystals from a system of given composition. As determination of the disappearance of a hydrate crystal resembles measuring bubble points (where disappearance of a last bubble of vapor from a system is observed), such data are called bubble point data. The infinite set of hydrate points in a given system forms the incipient hydrate - liquid - vapor equilibrium (H-Lw-V) curve. Although determination of the presence of a last hydrate crystal is usually done visually, Raman spectroscopy effectively replaced the human eye in the setup described here.

The Raman experiments were carried out in the Center for Hydrate Research at the Colorado School of Mines. A schematic diagram of the apparatus is given in Figure 3.1. The system was contained in a brass high-pressure cell equipped with a round sapphire glass window (1.5 cm diameter × 0.5 cm thickness).
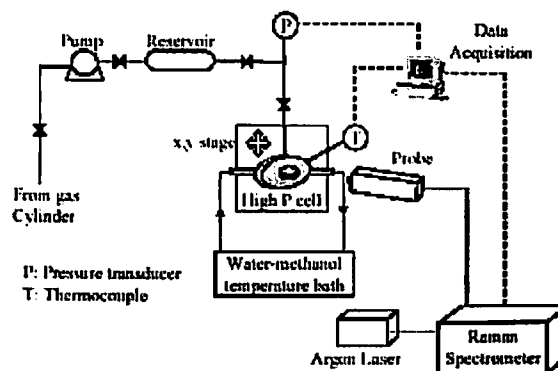
Figure 3.1. The Raman hydrate equilibria data apparatus

Source:J.A. Ripmeester, J.S. Tse, C.I Ratcliff, and B.M. Powell,

Nature, (1987)

The inner volume of the cell was approximately 1 cm^3. Coolant liquid was circulated through the body of the cell and the temperature was measured by a thermocouple inserted in the body of the brass cell. The tip of the thermocouple is approximately 4 mm removed from the actual system. The thermocouple was calibrated against a Fisher mercury thermometer. The error in the temperature reading is 0.2 K. The cell was mounted on a precision x, y-stage to facilitate controlling the position of the laser. The cell used in these experiments contained a magnetic steel bullet to allow for manual stirring of the solution during experiments.

The cell was equipped with a high-pressure connection to a gas reservoir system. The pressure in the cell was regulated by pumping a certain amount of gas into the system, using a Haskel gas booster pump. Note that Raman experiments were constant volume experiments. This means that the overall composition of the system changed: the pressure of the system was controlled by adding or releasing gas from the system. The pressure was measured using a Heise pressure transducer, with an error of 1 % of the measured value.

The presence of hydrates in the high-pressure cell was detected using a Raman spectrometer. Spectra were obtained from a Renishaw fiber optic based Raman spectrometer, using a 2400 grooves/mm grating. The excitation source was a 30 mW spectra Physics Argon ion laser. The frequency of the emitted light was 514.53 nm, corresponding to a wavelength of 19435.2 cm^{-1}. The spectrometer was calibrated using emission lines of Neon.

Table 3.1. Composition of studied processed natural gas

Composition (mol %)	
Methane	97.5275
Ethane	0.8797
Propane	0.1397
i-butane	0.0149
n-butane	0.0248
i-pentane	0.0180
n-pentane	0.0203
Hexane	0.0222
Heptane	0.0126
Nitrogen	0.9303
Carbon dioxide	0.4100

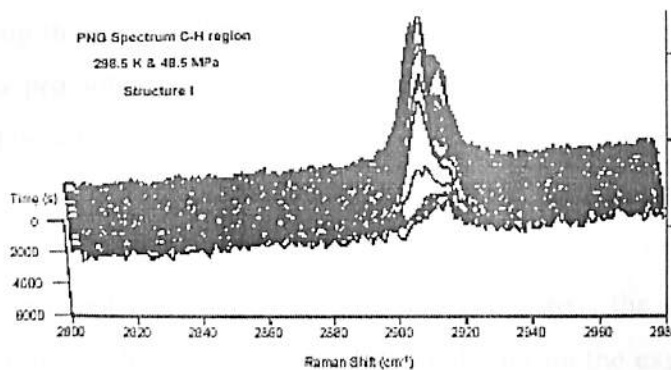Source: *J.A. Ripmeester, J.S. Tse, C.I Ratcliff, and B.M. Powell, Nature, (1987)*

Figure 3.2. A typical accumulation of Raman spectra
Source:*J.A. Ripmeester, J.S. Tse, C.I Ratcliff, and B.M. Powell,*
Nature, (1987)

An independent check on the calibration was the 546.074nm (183125 cm^{-1}) Hg line emitted by a common TL light. If properly calibrated, the spectral accuracy was 0.2

2005

cm^{-1}. The Raman spectra were collected real time together with pressure and temperature readings.

Two sets of hydrate point data were obtained: One data set was obtained for a system consisting of the processed natural gas (PNG) combined with an approximately equal molar amount of water. The composition of PNG is given in Table 3.1. The other data set was obtained for a system of PNG with a 6 mol% sodium chloride solution. The solution was prepared with a Mettler balance (0.1 mg precision) before it was added to the equilibrium cell. The cell was rinsed with this solution, after which 0.3 cm^3 of the prepared solution was loaded into the high-pressure cell. The rest of the volume was flushed 3 times with PNG to remove air from the system and finally filled with PNG to obtain the desired pressure.

The experimental procedure was as follows. Hydrates were formed at a constant pressure by decreasing the temperature of the cell. The water rich phase was not stirred during formation, to promote formation of hydrates only at the interface of the two phases. By limiting the presence of hydrates to the interface of the two phases, searching for the last hydrate crystal by moving the focal position of the laser was not needed.

An actual experiment consisted of equilibrium cell across the incipient 3-phase line, while the equilibrium cell was intermittently stirred. During the experiment, Raman spectra of the interface and pressure and temperature data were collected simultaneously. Typically, heating rates were around 0.1 K per 5 minutes. Crossing of the 3-phase incipient line was characterized by a disappearance of the hydrate Raman signal.

An example of spectra obtained during a typical experiment is given in Figure 3.2. The intense signals observed for the first 4000 seconds were generated by the presence of a hydrate phase. At that time, the hydrate phase dissociated and the remaining

weak signal is typical for hydrocarbons dissolved in a liquid water phase. The pressure and temperature at which the last notable contribution of hydrate was found, was taken as the incipient 3-phase condition.
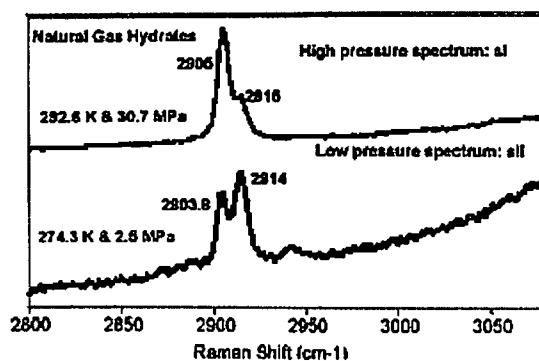

Figure 3.3. Raman spectra obtained from PNG hydrates

Source:J.A. Ripmeester, J.S. Tse, C.I Ratcliff, and B.M. Powell,

Nature, (1987)

The structure of the hydrate was taken from analyzing the exact contributions to the last hydrate spectra observed before the H-Lw-V line was crossed. These contributions can be compared to spectra that for example Sum et al. collected for sI and sII hydrates formed in methane rich environments.

3.3 Results and Discussion

Before the actual hydrate point data were collected, hydrates were formed at a low pressure and a high pressure in the equilibrium cell and Raman spectra were obtained from the hydrate phases. Predictions of the equilibrium curve showed that the system would supposedly form sII hydrates at low pressures, but that sI would be the most stable hydrate structure at pressures over 15 MPa. The hydrates were formed from distilled water and PNG, at the interface separating the two fluid phases. At a pressure of 2.5 MPa,

the temperature was decreased to the ice point and then heated to 274 K. The solid remaining in the sample was hydrate and a set of Raman spectra was obtained. The accumulation time used was 400 s. The hydrates were dissociated and ice was formed again, but now at a pressure of 30 MPa. The sample was heated to 293 K, the remaining solid being hydrate, and a second set of spectra was obtained. These spectra are shown in Figure 3.3.

The hydrates that are formed at the two different pressures were strikingly dissimilar. The main contribution was caused by light scattered from the C-H bond in methane molecules. The top spectrum was identified as methane occupying a sI hydrate. The contribution at 2905 cm^{-1} indicated methane present in the large cage ($5^{12}6^2$) and the contribution at 2915 cm^{-1} was for the small cage (5^{12}). The bottom spectrum is typical for a sII hydrate. The large ($5^{12}6^4$) and small (5^{12}) cage contributions were respectively found at 2904 cm^{-1} and 2914 cm^{-1}. The inversion of peak intensities reflected the different ratio of large to small cages in sI and sII. The fact that the methane contributions were the most significant was a qualitative indication that the methane is the most abundant guest, even in a sII hydrate. Slight contributions of ethane and propane occupying the hydrate are found as weak signals centered at 2890 cm^{-1} and 2940 cm^{-1}.

These Raman spectra were sufficient evidence to show that the water + PNG system formed both sI and sII hydrates: sII is the more stable structure at low pressures and sI at high pressure. In order to determine the conditions of the quadruple point sI-sII-Lw-V, hydrate point data were collected along the entire Lw-H-V equilibrium curve. This was done using the experimental method. As expected, the stable structure on the Lw-H-V curve was sI at high pressure and sII at low pressures, with the quadruple point estimated at 287.7 K and 12 MPa. The measured hydrate point data are given in Table 2.

Table 3.2. Collected hydrate point data

PNG + H₂O			PNG + H₂O + 6 mol% NaCl		
T(K)	P(MPa)	structure	T(K)	P(MPa)	structure
278.8	3.83	sII	268.0	3.68	sII
283.6	6.71	sII	274.4	7.21	sII
285.8	8.43	sII	279.1	13.95	sII
287.2	11.16	sII	282.1	22.38	sII/sI (?)
287.2	10.50	sI	283.9	28.59	sI (?)
287.5	11.81	sII/sI	284.3	31.12	sI
287.9	12.29	sII/sI	284.7	32.33	sI
288.7	13.51	sI	285.2	34.70	sI
290.4	16.67	sI	286.5	42.25	sI
292.8	23.48	sI	288.0	50.71	sI
294.6	29.83	sI	289.2	57.28	sI
295.8	34.25	sI			
297.3	41.92	sI			
298.5	48.51	sI			
299.5	54.67	sI			
300.4	60.87	sI			
301.3	68.23	sI			

Source: J.A. Ripmeester, J.S. Tse, C.I Ratcliff, and B.M. Powell, Nature, (1987)

Hydrate points were also determined for a 6 mol% sodium chloride present in the liquid and these data are also shown in Table 3.1. In general, the spectroscopic evidence suggested that dissociation of or transition to a certain structure could occur within a few minutes. It was not unusual to find contributions from the non-dominant structure in the spectra, only to lose these contributions rather suddenly as temperature approached the equilibrium value. This suggests that metastability did not play a significant role in the experiments.

All the hydrate equilibrium data measured in this work are shown in Figure 3.4. The open symbols show P, T conditions at which the last few observable spectra indicated the presence of sII hydrates. The filled squares and diamonds indicate that sI was stable near the equilibrium boundary. The presence of salt in the water phase shifts the equilibrium curve from 9.5 to 10.5 K to the left in a pressure –temperature diagram.

Notice that the slope dP/dT of the H-Lw-V curve is slightly higher if sodium chloride is present in the water phase. This phenomenon is commonly neglected, but significant when pressures are done over a wide pressure range.

As can also be seen, the quadruple points shifts to a higher pressure if the H-Lw-V curve shifts to a lower temperature due to the inhibiting effect of salt. This is a surprising result, especially when the data are compared to predictions generated from an in-house hydrate equilibrium program. The lines shown in Figure 3.4 represent prediction results and those suggest that the pressure at which the hydrate phase transitions from sII to sI is virtually independent of temperature. This discrepancy is unexpected as the prediction of the quadruple point for the system without sodium chloride coincides with the data. But for the system containing sodium chloride, either the prediction or the experimental determination of the quadruple point is wrong.
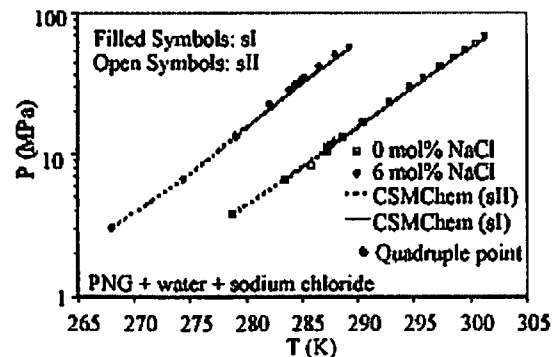
Figure 3.4 P, T diagram of collected hydrate point data

Source:J.A. Ripmeester, J.S. Tse, C.I Ratcliff, and B.M. Powell,

Nature, (1987)

The evidence supporting the experimental observation of the quadruple point with salt is given in Figure 3.5. Several of the spectra collected for the determination of the quadruple point at 282.1 K and 22.38 MPa are shown. From the spectra it is clear that sII is the hydrate structure that was stable at the start of the experiment. As the equilibrium point is approached, the contribution from sII becomes weaker and signal at 2905 cm^{-1}, typical for sI becomes stronger. Then, in the few minutes it takes to heat the equilibrium cell from 0.2 K to 0.1 K below the equilibrium point, the sI hydrate contribution to the spectrum increases quite dramatically. One would consider sI to be the stable structure at the boundary, but since sII persisted until the boundary was reached, this particular evidence was interpreted as a quadruple point.

However, the spectra measured at 28.6 MPa were not too dissimilar from what is shown in Figure 3.5; so, the actual quadruple point can be considered to occur at an even higher pressure (28 MPa), depending on how one interprets the spectra. In any case, it is clear that the quadruple point is not located at a pressure of 14 MPa, as was suggested by the prediction.

The evidence supporting the prediction of the quadruple point for the system with salt is shown in Figure 3.6. The evidence is related to the question why a system of constant composition forms a different hydrate structure at higher pressures.

Raman Shift (cm-1)
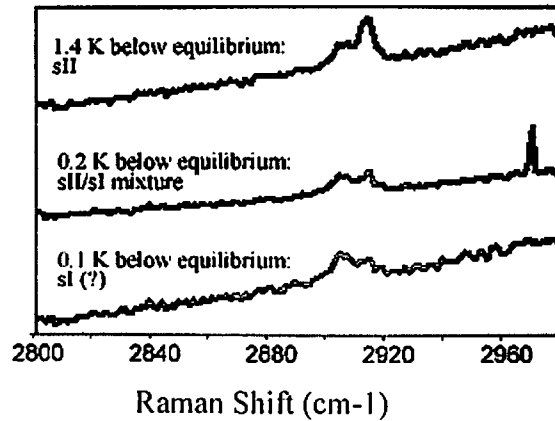
Figure 3.5. Raman evidence for the quadruple point of the

system PNG + water + 6 mol% NaCl

Source:J.A. Ripmeester, J.S. Tse, C.I Ratcliff, and B.M. Powell,
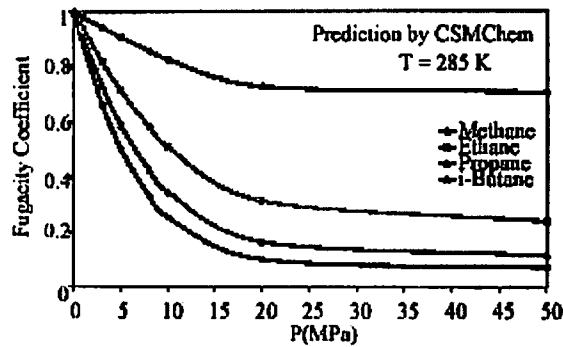
Nature, (1987)

Figure 3.6. Guest fugacities determine hydrate structure and

show why transitions are predicted around 10 MPa

Source:J.A. Ripmeester, J.S. Tse, C.I Ratcliff, and B.M. Powell,

Nature, (1987)

35   2005

The explanation is straightforward. As the pressure increase, the fugacity coefficients of the main hydrate formers are reduced. The fugacity coefficients of the main sII formers, ethane, propane and i-butane are much more reduced than the fugacity coefficient of methane. This means that at a low pressure, the fugacities of all guests resemble what their fugacity would be in an ideal gas mixture. At higher pressures, the sII formers behave much more like they are present in a liquid hydrocarbon phase, even though PNG is of course supercritical. The reduced fugacities of the sII formers mean that sII is less likely to be occupied by those guests and becomes unstable with respect to sI hydrate. For systems where the concentration of the superior sII formers propane and i-butane are fairly low, this will result in a structural transition occurring at some higher pressure. Our calculations indicate that any system in which the combined concentration of propane and i-butane is lower than 0.5%, a structural transition will occur at some pressure lower than 70 MPa.

Figure 3.6 shows that the change from low-pressure to high-pressure behavior is mainly located in the 10 to 15 MPa region. Given that this behavior is fairly independent of temperature – the same picture emerges if calculations are done at 275 K or 295 K - this means that for a system of given composition, the exact position of the transition will be independent of temperature. Thus, any prediction program that determines the hydrate stability from guest fugacities will predict that the structural transition occurs at approximately the same pressure, independent of the amount of inhibitor present in the system. The reasoning seems solid, except that the conclusion is in flagrant contradiction with the data observed in this work.

It is clear that Raman spectroscopy can indeed be used to measure hydrate point data and determine hydrate structure simultaneously. However, the determination of hydrate structure can sometimes be ambiguous, in this case probably because the intensity of the hydrate spectra was adversely affected by the presence of the inhibitor.

Even then, the discrepancy between the measured and calculated quadruple point for the system with salt indicates that either the experimental method needs further refinement, or that our understanding of the relative stability of sI and sII hydrates is wrong.

3.4 Inferences

The main result of this work is that Raman spectroscopy can be used to carry out hydrate phase equilibrium measurements with simultaneous detection of the hydrate structure. A hydrate Raman spectrum can be used to detect the dissociation of a hydrate in a regular phase equilibrium experiment. The structure identification in such an experiment is based on the fact that sI and sII Raman spectra can differ due to the different confinement of the guests in the hydrate cavities.

The Raman method has been used to determine hydrate point data for a system containing a processed (methane enriched) natural gas, water and 0 and 6 mol% sodium chloride. It is generally assumed that natural gases form sII hydrates. However, this particular system was found to form sII hydrates at pressures below 12 MPa. And sI hydrates above that pressure. For the system without salt, the quadruple point sI-sII-Lw-V was found at 287.7 K and 12 MPa. For the system with 6 mol% salt relative to Water, the quadruple point was found at a higher pressure, i.e., 282.2 K and 22.4 MPa. However, this experimental observation is in doubt, as a prediction tool that otherwise predicts the data within 6 % suggest that the quadruple point pressure should be independent of the concentration of inhibitor in the system.

Nonetheless, it is clear that ignoring the possibility of sI formation in natural gas systems is misleading. Any natural gas that has a combined concentration of propane and i-butane of less than 0.5 mol% will have a quadruple point pressure lower than 70 MPa. This means that such gases only form sII if the pressure is lower than their quadruple

point pressure. The capability to predict hydrate structure will become ever more crucial to ensure that flow assurance strategies are based on the actually occurring hydrate structure.

CHAPTER-4
HYDRATE CONTROL

4 Gas Hydrate Control

The first approach to preventing hydrate formation is dehydration, which can be performed through the use of solid desiccants or by normal glycol dehydration. Unfortunately, no process can achieve complete dehydration for economic and/or operative reasons. Another tactic is to keep the system out of the hydrate formation conditions. This method is known as thermodynamic inhibition and involves several approaches.

Thermodynamic inhibition can be achieved by heating the system beyond the hydrate formation temperature at a given pressure, using insulation to keep temperature from dropping into the vulnerable zone, depressurizing the system, or injecting inhibitors such as methanol, glycol, or salt solutions such as potassium formate. The first three methods are often technically impractical, or very costly. At best, they are typically used in conjunction with complementary methods.

Thermodynamic inhibitors are chemical compounds added in high concentrations (10-60wt. %), to alter the hydrate formation conditions, allowing hydrates of the new mixtures form at lower temperatures or higher pressures. Using thermodynamic inhibitors implies regeneration units, which involves higher operating costs. Handling of methanol (the most effective thermodynamic inhibitor) is complicated because of its toxicity and flammability. Furthermore, methanol contamination of the hydrocarbon can compromise the value of the product and give downstream processing problems. Ethylene glycols such as mono-ethylene glycol (MEG) are less flammable, and reduce losses, but are more expensive and less available than methanol. Salt solutions might be used in hydrate inhibition but they are corrosive, less effective than methanol or glycols, and could cause scale deposits in the process equipment.

Recently, a new technique, independent of the thermodynamic conditions, which requires low doses of chemical compounds to inhibit hydrate formation, is being developed. Two classes in particular are known as low-dosage inhibitors. The class referred to as *kinetic inhibitors* delays the nucleation and growth of hydrate crystals for substantial periods of time. The second class of inhibitor prevents agglomeration of hydrate crystals so that transportable slurry is maintained. This class is known as the anti-agglomerants.

4.1 Hydrate Control through Water Removal
(Water Dew Point Lowering)

The initial technique to control hydrates is to remove the host water molecules (or sufficient guest molecules) causing hydrate instability. The removal of the guest molecules is depressurization which is not desirable due to the flow interruption. With respect to removal of host molecules, however, the following passage, stated by Deaton and Frost over half a century ago: is still true today

"The only method found to be completely satisfactory in preventing the formation of hydrates in gas transmission lines is to dehydrate the gas entering the line to a dew point low enough to preclude formation of hydrates at any point in the system."

Two common misconceptions exist concerning the presence of water to form hydrates in pipelines. The first and most common misconception is that a free water phase is absolutely necessary for the formation of hydrates. The second misconception is that ice
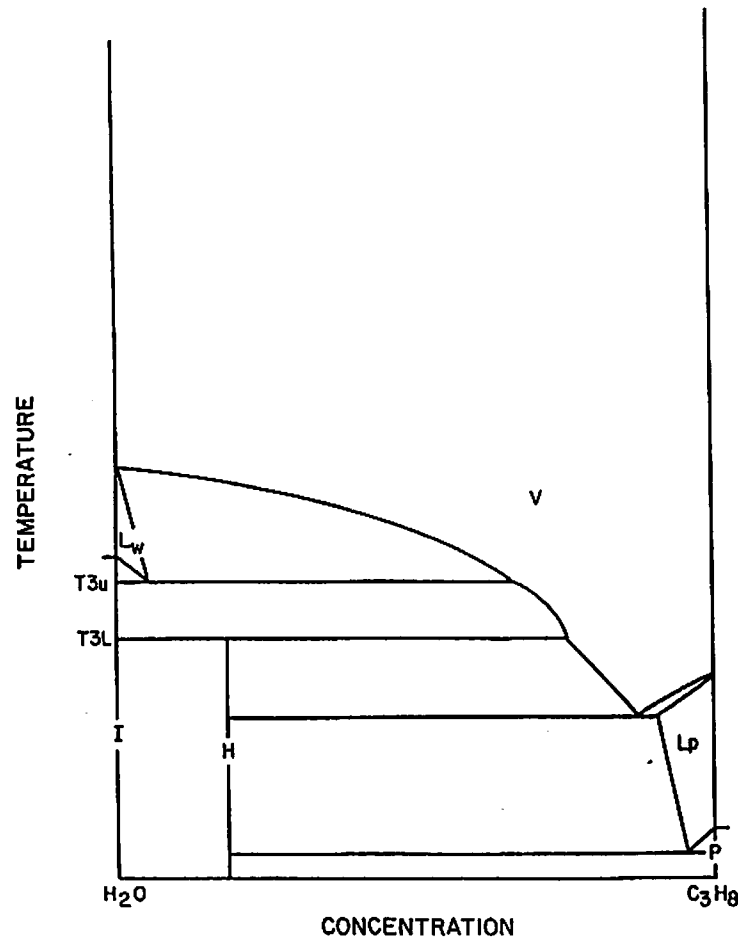
Figure 4.1 *Isobaric Temperature-Composition Diagram for Propane + Water*
Source: *Clathtrate Hydrates of Natural Gases, Sloan(1998)*

is the solid phase in equilibrium with temperatures below the hydrate point. Figure 4.1 serves as visual confirmation that, below T3L it is thermodynamically feasible to have H-V and H-L$_{HC}$ equilibrium, and that ice is the correct condensed water phase only over a small temperature range (between T3u and T3L) of the phase diagram.

In addition there have been multiple studies (Sloan et al. 1976; Cady 1983 Woolridge et al. 1987; Kobayashi et al. 1987) which demonstrate that hydrate growth can

41   2005

easily occur from a hydrocarbon phase if a hydrate nucleus or free water is either already present, (2) adsorbed on a wall, or (3) on a third surface. If any incident upset caused free (or adsorbed) water to exist, the water will likely convert to hydrate, and continue to grow to the point of flow obstruction.

·The second common misconception is that, if two phases (hydrocarbon and a condensed water phase) exist at low temperatures, the solid phase will be ice (Buck et al. 1985). Figure 4.1 shows that ice the incorrect water condensed phase in equilibrium with hydrocarbon over most of temperature range.

The maximum water content of gas is specified as 7 lb_m/MMSCF, or as 4 lb_m/MMSCF in colder regions. After the free water is separated from the gas stream two processes are commonly used to lower the dew point by removing dissolved water. These two processes have evolved from the earlier three types suggested by Deaton and Frost 1) hygroscopic solutions, 2) chemical adsorption by solids, and 3) physical adsorption by solids,. In the first process, the water concentration lowered by contacting the gas with tri-ethylene glycol (TEG), which absorbs w, through hydrogen bonding. The second process is not in current use because economics prohibited non-regenerative solid chemical adsorbants. In the third process the gas is contacted with a solid, such as molecular sieves, alumina, or silica gel, which selectively adsorbs water.

In the first process, the hygroscopic liquid TEG absorbs water from the gas in a tray or packed column. Then the TEG is transferred to a regenerator to remove (strip) the water before recycling TEG to the absorber. The hydrogen bonding of water TEG is effective, so that only two or three ideal equilibrium stages are required for absorber, with circulation rates of 2 to 5 lb_m glycol/(lb_m water removed). However, overall tray efficiency is typically 25% to 35% resulting in an absorber with 8 to trays. Gas Processors Association Handbook, 1987). Bucklin et (1985) have used TEG for control

of hydrates in Arctic conditions, for water cone as low as 0.05 lb_m/MMSCF or a dew point of -60°F.

Within ten years of Hammerschmidt's 1934 discovery of hydrates in pipelines, he and his colleagues published details of gas dehydration with solid dessicants. In general, solid dessicants are placed in parallel packed bed adsorbers through which gas is passed. One adsorber is used to remove water from the gas, while the parallel unit is either being regenerated via high temperature desorption into inert gas, or cooling. There are a number of solid dessicants, but the more common ones, in order of decreasing drying efficiency, are molecular sieves, silica gel and alumina. Table 4.1 presents a comparison of dew points achievable and properties of the three solid dessicants.

The use of molecular sieves has become the dominant adsorbent due to advantages of extremely low dew points, high adsorption of water (rather than large amounts of hydrocarbon) and, unlike silica gel, molecular sieves are not damaged by liquid water. Molecular sieves are crystalline solids which provide the lowest dew points commonly obtainable and they are typically used in low temperature processes such as turboexpander plants, where the requirements are very stringent (as low as 0. 1 ppm). Molecular sieves are designed to adsorb particular molecules based upon polarity and size. With decreasing selectivity sieves adsorb water, alcohols, glycols, hydrogen sulfide, and carbon dioxide, while sieves adsorb mercaptans and heavy organics less, based upon molecular size.

Nielsen and Bucklin (1983) determined that methanol injection offers economic advantages, both relative (1) activated alumina for incoming gases with 4 lb_m H_2O/MMSCF, and (2) molecular sieves for incoming gases with 23 lb/MMSCF in a turboexpander plant application. However for low temperature processes, such as

43

turboexpander discharge temperatures less than $-150°F$, normal practice is to dehydrate via molecular sieves.

Table 4.1 Properties of Solid Dehydration Agent

Property	Molecular sieve	Silica gel	Activated alumina
Range of dew Points. °F	-150 → 150	-80 → 120	-100→ 130
Typical water	Capacity	(lb_m H_2O / 100 at 298 K	100 lb_m adsorbent)
10% Relative Humidity	20	6	5
20% Relative Humidity	21	10	7
30% Relative Humidity	22	15	9
40% Relative Humidity	22.5	20	11
Major adsorbent	Constituents	(% dry basis)	
SiO_2	40-42	99.82	
Al_2O_3	33-36		95+
Surface area(m^2/g)	600-800	750-800	200-350
Porevolume(cm^3/g)	0.28	0.43	0.21-0.34
Avg. pore dia.(°A)	3,4,5,6,8 & 10	22	26-41
Cost($/$lb_m$)	1.3-1.8	0.48	0.21-0.605

Source: modified from Hales, 1982

4.2 Hydrate Control through Heating

In Figure 4.2 consider a trace of the second method of hydrate control - through heating at constant pressure. First consider the case for which hydrate formation has occurred with excess gas, so that all of the free water has been converted to hydrate and the system consists of only vapor and hydrate in equilibrium at point A. The object of heating, depressurization, and inhibitor injection is to move the system from point A (vapor-solid region) across the three-phase (L_W-H-V) line into the fluid (vapor liquid) region. If hydrate formation occurs from a gas and a free water phase, the starting conditions for dissociation will be determined by the three-phase line.

Heat input may occur at constant pressure to the vapor and hydrate, causing movement from Point A to the three-phase equilibrium line at Point B. This transition is called sensible heat input because no phase transition occurs until point B is reached, where the first drop of free water appears as a result of hydrate dissociation. At Point B, all energy input is spent on hydrate dissociation at constant temperature at pressure. The heat of hydrate dissociation is always much greater than sensible heat. As more hydrate dissociated, the phase amounts of gas and liquid increase until the complete disappearance of the hydrate.

After the hydrate is dissociated, sensible heat input causes the remaining vapor, and liquid phases to progress to Point C. The operator may then wish to remove the free water phase using mechanical means, such as a pipeline "ball," "sphere," hydrates will re-form much more easily if free water previously contained hydrates, because water retains a significant amount of residual hydrate structure.

It is often difficult to locate a pipeline hydrate plug to begin heating. After the plug is located, heating to dissociate a hydrate plug must be done with caution, beginning

from the ends and progressing toward the middle of the plug. If a hydrate plug is dissociated in the middle, the undissociated hydrate at either end may enclose an exponentially increasing pressure with an increase in temperature. The result may be equipment wall failure, blowouts, or hydrate projectiles in pipelines.
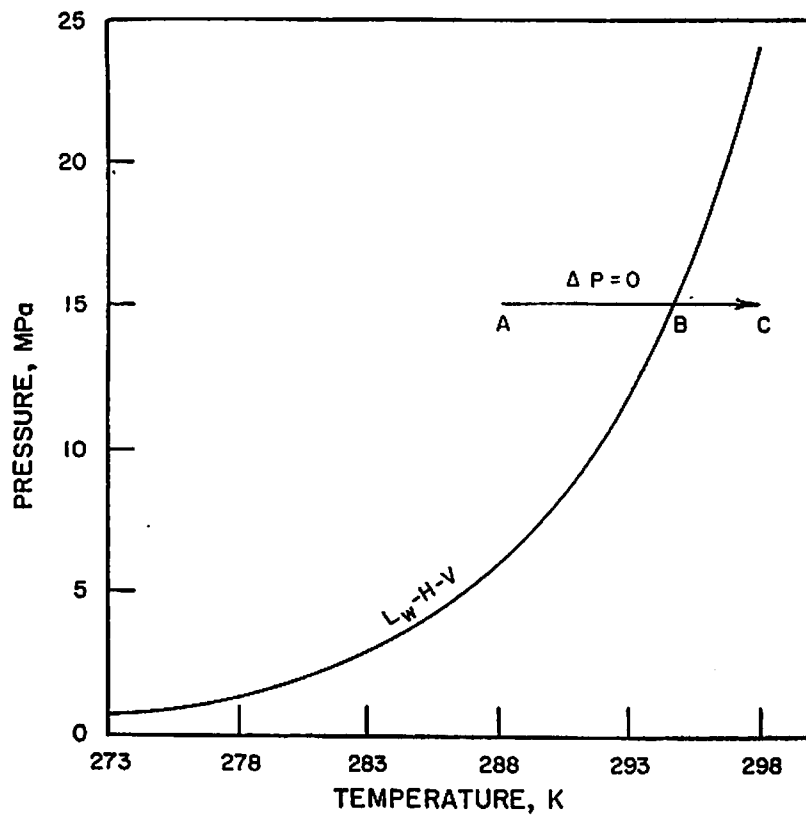
Figure 4.2 Isobaric heating from the vapor-hydrate region (A) across

the three phase line into the vapor-liquid water region(C)

Source: Clathtrate Hydrates of Natural Gases, Sloan(1998)

One possibility of removing hydrate plugs (Hale, 1988) which can be reached by flowing chemicals is to use small amounts of aqueous chemicals with a high exothermic heat of reaction, such as those indicated by Ashton et al. (1986). The reaction combines sodium nitrite ($NaNO_2$) and ammonium nitrate (NH_4NO_3) or ammonium chloride (NH_4Cl) as follows:

$$NaNO_3 + NH_4NO_3 \rightarrow N_2 + 2H_2O + NaNO_3 \qquad (1)$$
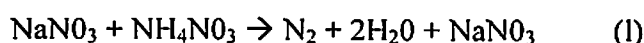
A three molar solution of the above reactants produces 400 SCF (11 m^3) of nitrogen gas and 132,500 BTU's (879 MJ/m^3) of heat per barrel of solution. The sodium nitrate produced gives a brine that is equivalent to a 9.7 lb_m/gal (1152 kg/m^3) sodium chloride solution. If such chemicals can be reacted in the vicinity of a hydrate plug, then the heat generated will dissociate the hydrate. As a caution, Dewan (1989) noted also that the reaction generates nitrogen, which may add to the exponential increase in gas pressure, as the temperature increases for hydrate dissociation. While the above method appears promising, it has not been used industrially.
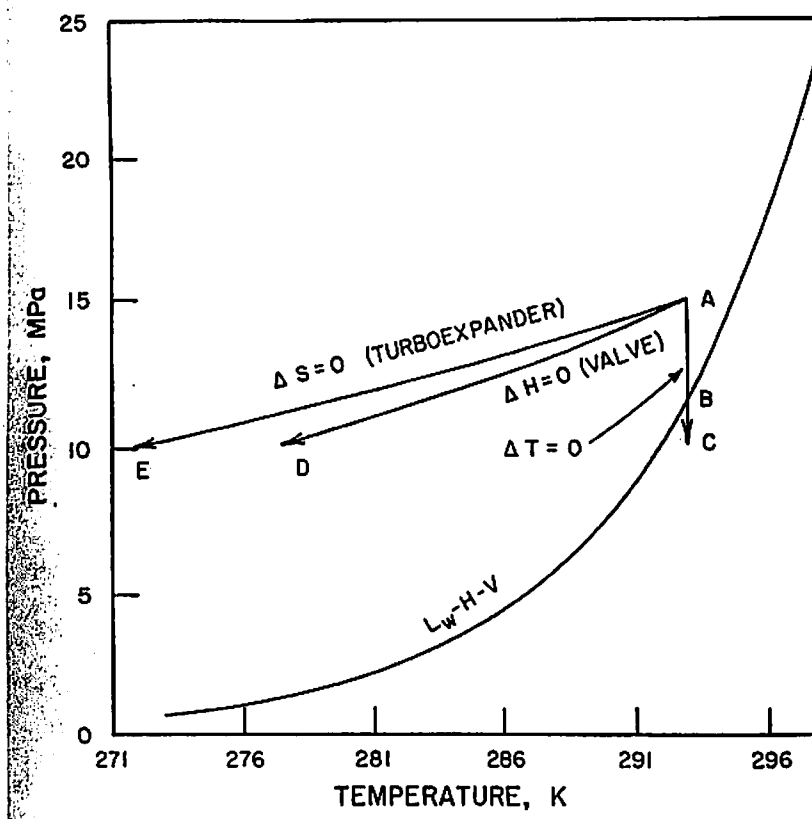
Figure 4.3 Isothermal, Isenthalpic (ΔH=0), and Isentropic (ΔS=0)
Depressurization from the Vapor-Hydrate Region.
Source: Clathtrate Hydrates of Natural Gases, Sloan(1998)

4.3 Hydrate Control through Depressurization

There are three limiting cases of pressure reduction to control hydrates: (1) isothermally, as with infinitely slow pressure reduction, (2) isenthalpically, as with rapid pressure reduction without heat transfer (Joule-Thomson expansion), and (3) isentropically, as with pressure reduction through an ideal turboexpander without heat transfer. The three processes are shown for similar pressure drops, beginning from point A in Figure 4.3.
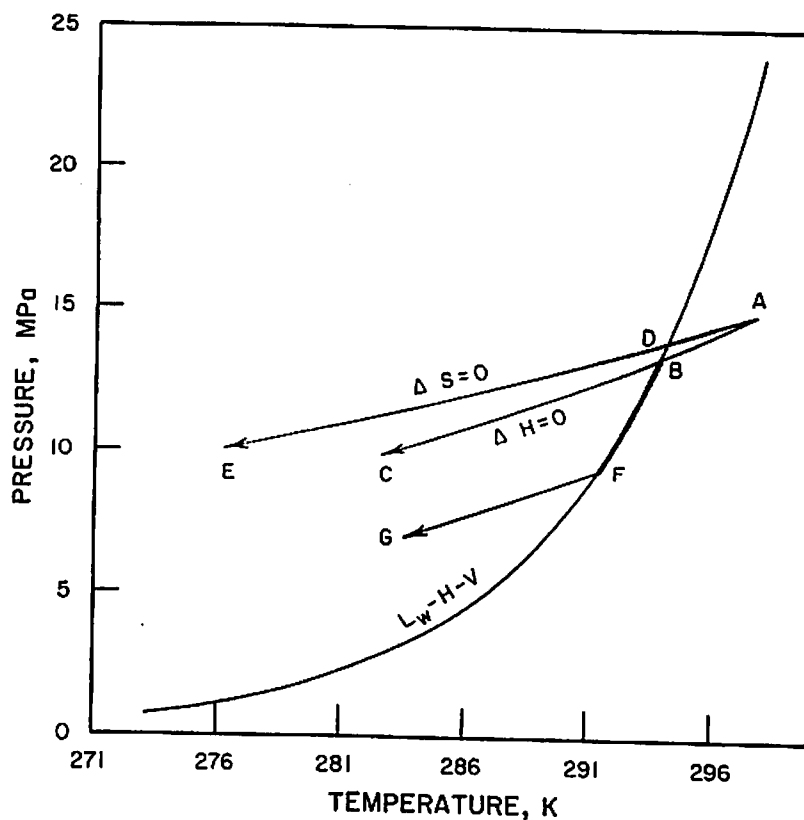
Figure 4.4 The Effect of Hydrate Dissociation (ABFE) upon Ideal (ABC)
Isenthalpic ($\Delta H=0$) Depressurization with Ideal Isentropic ($\Delta S=0$)
Depressurization from the Vapor-Liquid Water Region.
Source: Clathrate Hydrates of Natural Gases, Sloan(1998)

It is assumed (1) that initially, only vapor and hydrate are present at Point A and (2) that hydrate formation ceases with depletion of free water. If hydrate formation occurs without subcooling from free water, the system initially is at the three-phase (L_w-H-V) condition but the processes will progress in a similar manner to those described

'A common misconception about hydrate depressurization is that depressurization alone can cause dissociation. From a First Law of thermodynamics analysis, since the dissociated hydrate components have more energy in the vapor and liquid than they do in the hydrate, energy to promote hydrate dissociation must be derived from the surroundings, e.g., the ocean floor, air, heat exchangers, or the hydrate itself. The fundamental purpose of depressurization is to decrease the pressure at the hydrate interface, so that the hydrate equilibrium temperature is below the surroundings. The temperature gradient from the surroundings causes heat input and hydrates dissociation.

Optimally one should depressurize a hydrate plug simultaneously from both ends. If only one end of a plug is depressurized, the pressure gradient across the dislodged plug may cause a pipeline hydrate projectile with enough momentum to cause damage and safety problems at bends and elbows. As a consequence it is important to prevent a large differential pressure across the hydrate plug.

Isothermal hydrate depressurization represents a upper thermal limit to the expansion, shown as a vertical line in Figure 4.3. With isothermal pressure reduction the process is extremely slow, making it impractical from an industrial perspective. A pressure is reduced; sensible heat is supplied from the surroundings to both the hydrate interface and vapor phases to maintain the temperature while the system moves from Point A to Point B. At Point B the hydrate begins to dissociate and heat of hydrate dissociation is input to maintain constant temperature until dissociation is complete, so

that further pressure reduction causes the system to progress toward Point C, requiring only sensible heat input to vapor and liquid phases.

In Figure 4.3 the isentropic ($\Delta S=0$) depressurization at line AE represent an extreme lower temperature limit achieved only through system reversibility, via a ideal machine (e.g., turboexpander) which produces work A more common process pressure reduction is the isenthalpic ($\Delta H = 0$) process which occurs with rapid depressurization in the absence of heat exchange, as shown in line AD of Figure 4.3 For rapid hydrate dissociation in a flow system, neither heat (Q) nor shaft work (W_s) is normally exchanged with the surroundings, so the enthalpy change is zero by the First Law of thermodynamics for a system at steady state ($\Delta H=Q-W_s$). Relative to the isenthalpic case, any heat input to the system will cause the temperature to increase while any work removed from the system will cause the temperature to decrease.

The isenthalpic limit is normally called a Joule-Thomson expansion. The pressure versus temperature slope of the Joule-Thomson isenthalpic expansion curves are much less than the three-phase (L_w-H-V) equilibrium curves. Therefore, with isenthalpic pressure reduction the gases will expand further into the hydrate region, as shown starting from Point A in Figure 4.3, or toward the three-phase (L_w-H-V) equilibrium line from the vapor-liquid region, as from Point A in Figure 4.4. Rapid isenthalpic expansion alone, therefore Promotes hydrate formation by cooling of the gas.

As shown in line AD of Figure 4.3, surroundings heat will be required to increase the system temperature to a value beyond the three-phase line, usually at constant pressure because the hydrate is not confined. Isenthalpic expansion alone will not cause hydrate suppression or removal. The limit to hydrate-free isenthalpic expansion from the vapor-liquid region, i.e., the point at which hydrates begin to form, is demonstrated in Figure 4.4 by the intersection of the $\Delta H=O$ line ABC with the three-phase (L_w-H-V) line.

In the depressurization process shown in Figure 4.4, while line ABC may be realized in the gas phase, the line does not represent conditions at a potential hydrate fluid interface. As the system is cooled to point B, a significant amount of hydrates may form if the system is not subcooled.

In Figure 4.4, once hydrates have formed (Point B), further depressurization will cause hydrate dissociation until that phase is depleted. In a direct analog to the depressurization of the Messoyakha Hydrate Field temperature at the hydrate interface will decrease along the three phase line BF as the pressure is decreased. The pressure decrease will result in lowering the temperature of the hydrate mass, and heat of dissociation will be drawn from the hydrate phase, and the produced water due to their higher thermal conductivities. As the hydrate is depleted at point F, depressurization will proceed isenthalpically along line FG .

However on pipeline plug dissociation, when the temperature of formation B is close to the ice point (e.g., ocean-bottom temperatures) hydrate dissociation may result in ice formation by removing heat from the hydrate mass. This is undesirable, because an ice layer is more difficult to dissociate (through heat input alone) than a hydrate layer which can be dissociated via both pressure reduction and heat input.

As a consequence it is prudent to decrease the pressure on a hydrate plug by only a few atmospheres to a pressure with an equilibrium temperature just above the ice point so that more rapid dissociation can be achieved Yakushev and Istomin (1991), Gudmundsson and Parlaktuna (1992), and Lysne (1995) indicate that dissociated water from hydrate can easily be converted to ice. Ice forms a protective cladding which inhibits further dissociation, both by thermal insulation and by mechanical flow blockage.

On the other hand, the gas processor may purposely choose to lower the water dew point of the gas via hydrate formation upon isenthalpic expansion, combined with refrigeration of the incoming gas. The solid hydrates are accumulated in a separator immediately after the expansion *valve*. This technique is called the LTX (low temperature expansion) process and may be viable when pressure drop is not a concern or when high pressure is economically available (Dorsett, 1989).

4.4 Hydrate Control through Thermodynamic Inhibition

Thermodynamic inhibitors (typically methanol or monoethylene glycol) are injected into processing lines as a means of hydrate control by breaking hydrate hydrogen bonds and by competing for available water molecules. Salts are used infrequently, due to corrosive properties and very low vapor pressures which keep them either in the aqueous phase or precipitated at the solubility limit. While ammonia is more than twice as effective as methanol on a weight basis, ammonia is seldom used (Deaton and Frost) due to the reaction of NH_3 with CO_2 in the gas to form solid plugs of ammonium carbonate, bicarbonate, and carbamate, which are more difficult than hydrate plugs. The handling of ammonia is a safety consideration.

The use of inhibitors shifts the three-phase (L_w-H-V) equilibrium curve to higher pressures and lower temperatures, as shown in Figure 4.5, by relative positions of the solid (inhibited) line to the dashed (uninhibited) line. While Figure 4.5 is for the unusual case of excess water, the diagram is identical for the typical case of excess gas. The parallel nature of the uninhibited and inhibited lines indicates the reason for the neglect of the pressure effect upon hydrate temperature depression. The effect of adding the inhibitor is to shift the three-phase equilibrium curve lowers than the process temperature at a given pressure. With inhibition in either Figure 4.2 or 4.3, Point A would exist in the vapor-liquid water region rather than the vapor-hydrate region.

Figure 4.5 may also be used to show that the hydrate temperature depression, ΔT, is always less than the ice temperature depression, ΔT' at the same inhibitor concentration, regardless of the inhibitor. Nielsen and Bucklin (1983) indicate
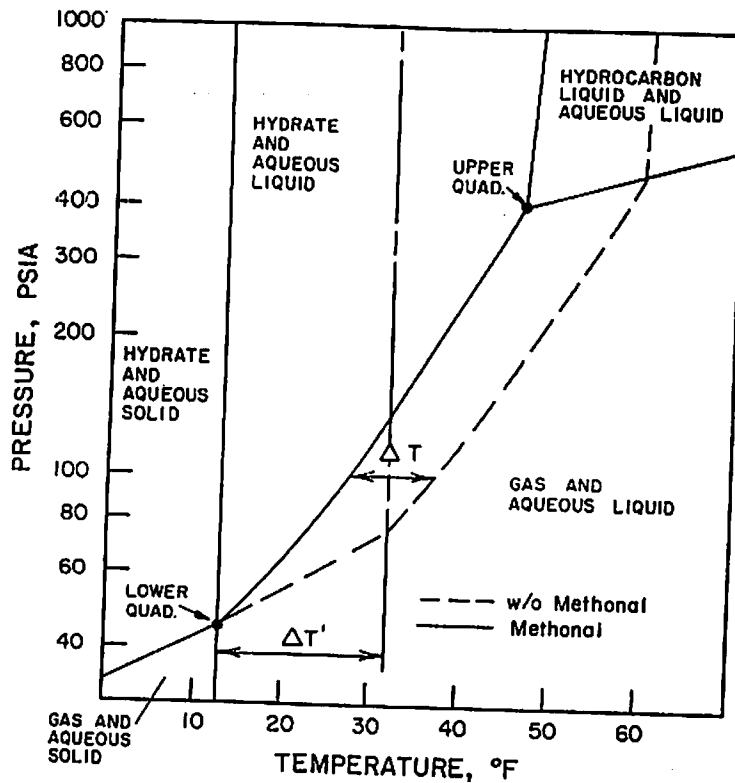
Figure 4.5 The Relative Freezing Point Depression of Methanol on Ice (ΔT')
and Hydrate (OT)_ (Reproduced, with permission, from Hydrocarbon
Processinu (Nielsen and Bucklin. 1983), by Gulf Publishing Co.)
Source: Clathtrate Hydrates of Natural Gases, Sloan(1998)

relationship of the two temperature depressions is given by:

$$\frac{\Delta T}{\Delta T'} = \frac{\Delta H(L_w \Leftrightarrow I)}{\Delta H(L_w + V \Leftrightarrow H)} - \frac{\Delta H(L_w + V \Leftrightarrow H) - \Delta H(I + V \Leftrightarrow H)}{\Delta H(I_w + V \Leftrightarrow H)}$$

by substituting in ΔH for hydrate formation from either ice or water in a ratio of about 0.35:

$$\Delta T = \Delta T'\left(1 - \frac{\Delta H(I + V \Leftrightarrow H)}{\Delta H(L_w + V \Leftrightarrow H)}\right) \approx 0.65\ \Delta T' \qquad (2)$$

where M and W are the molecular weight and the weight percent of the antifreeze agent, respectively. Nielsen and Bucklin (1983) indicate that for glycols, a cancellation of errors enables the Hammerschmidt equation to fit up to a mol fraction of 0.4. Townsend and Reid (1978) suggest that the original Hammerschmidt Equation (8.3) adequately represents depressions up to 60 wt% for ethylene glycol, and up to 75 wt% for diethylene glycol if the constant 2,335 is changed to 4,000. Nixdorf and Oellrich (1996) have recently shown that the Hammerschmidt equation provides a conservative prediction for natural gas systems inhibited with triethylene glycol (TEG).

Nielsen and Bucklin (1983) suggest that for methanol Equation (8.3) may be corrected for solutions above 20 wt%, for systems operating as low as 166.5 K for hydrate control by:

Whether methanol or glycol is used for hydrate depression, there are three possible phases into which the inhibitor may distribute. Figure 8.6 provides an

illustration of a tank which separates the three fluid phases, as follows:
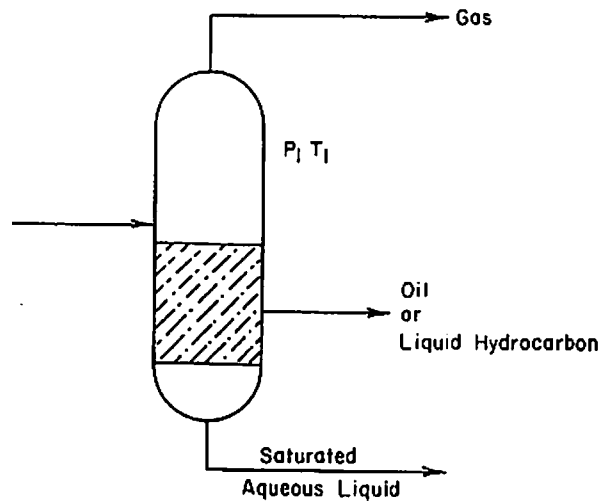
Figure 4.6 Three phase separator for vapor, liquid hydrocarbon, and aqueous phases

Source: Clathtrate Hydrates of Natural Gases, Sloan(1998)

1. The free aqueous phase where the hydrate inhibition occurs,

2. The vapor hydrocarbon phase, where the inhibitor may be lost, as in the usual case of methanol injection, and

3. The liquid hydrocarbon phase, which has appreciable solubility for both glycol and methanol and will cause inhibitor loss

All three phases are commonly present. As shown in the examples be significant fraction of inhibitor is lost due to partitioning into the non-aqueous phases where recovery is not economical.

Normally the hydrocarbon phase fractions are calculated assuming the vapor-liquid hydrocarbon phase envelope is not affected by the presence of the phase due

to the low solubility of water in the hydrocarbon liquid and the low pressure of water. This universal simplification allows calculation of hydrate for with knowledge of the vapor phase composition.

The loss of inhibitor to the vapor phases may be determined from Figure 4.7 from Nielsen and Bucklin (1983) for methanol at low temperatures or at temperatures in Figure 4.8 from Ng and Chen (1995), where K_v is the methanol mole fraction divided by that in the aqueous phase. The corresponding chart for losses from glycols at low temperatures is given in Figure 4.9 of Polderman (1958).

Heavier molecular weights of the glycols result in lower vapor pressures, glycol vaporization losses are less than methanol losses. Townsend and Reid indicate that ethylene glycol vaporization losses will be negligible at temperatures below the ice point when the operating pressure is above 5.17 MPa. Vapor losses will be still less at these conditions with di- or tri-ethylene glycol with molecular weights than ethylene glycol.

The low temperature solubility of inhibitors in liquid hydrocarbons is pre for methanol at low temperature in Figure 4.10 while solubility data for higher temperature and Figure 4.11 from Ng and Chen (1995), where K_{LHC} is the methanol mol fraction in the liquid hydrocarbon divided by that in the aqueous phase. Glycol solubilities in liquid hydrocarbons are given in Figures 4.12 and 4.13. Note that each of these figures only approximates the natural gases liquids.

The methanol concentration is normally >= 98 wt% prior to injection, while the ethylene glycol injection lines typically are in the range 65-75 wt%. Most of the ethylene glycol injected will remain in the liquid phase after injection. At cryogenic temperatures, Nielsen and Bucklin indicate that methanol is injected at a rate

such that the concentration in any process/pipeline free water will be 90 wt%, and the minimum recommended hydrate depression is the calculated depressed hydrate point plus 35°F, a safety factor.
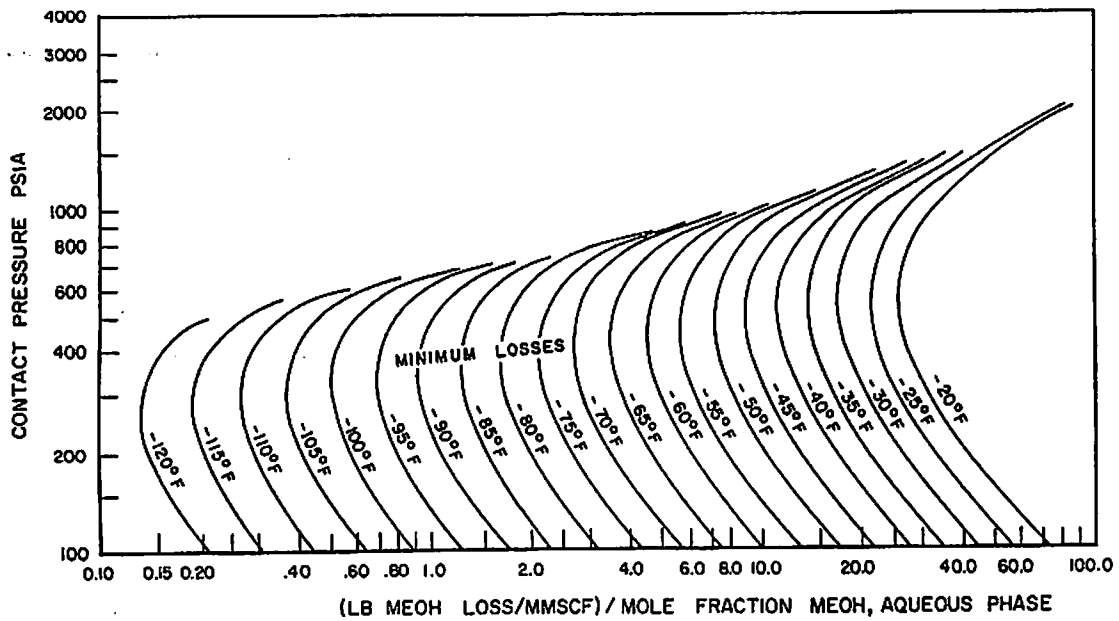
Figure 4.7 Loss of methanol to the vapor phase

Source: Clathtrate Hydrates of Natural Gases, Sloan(1998)
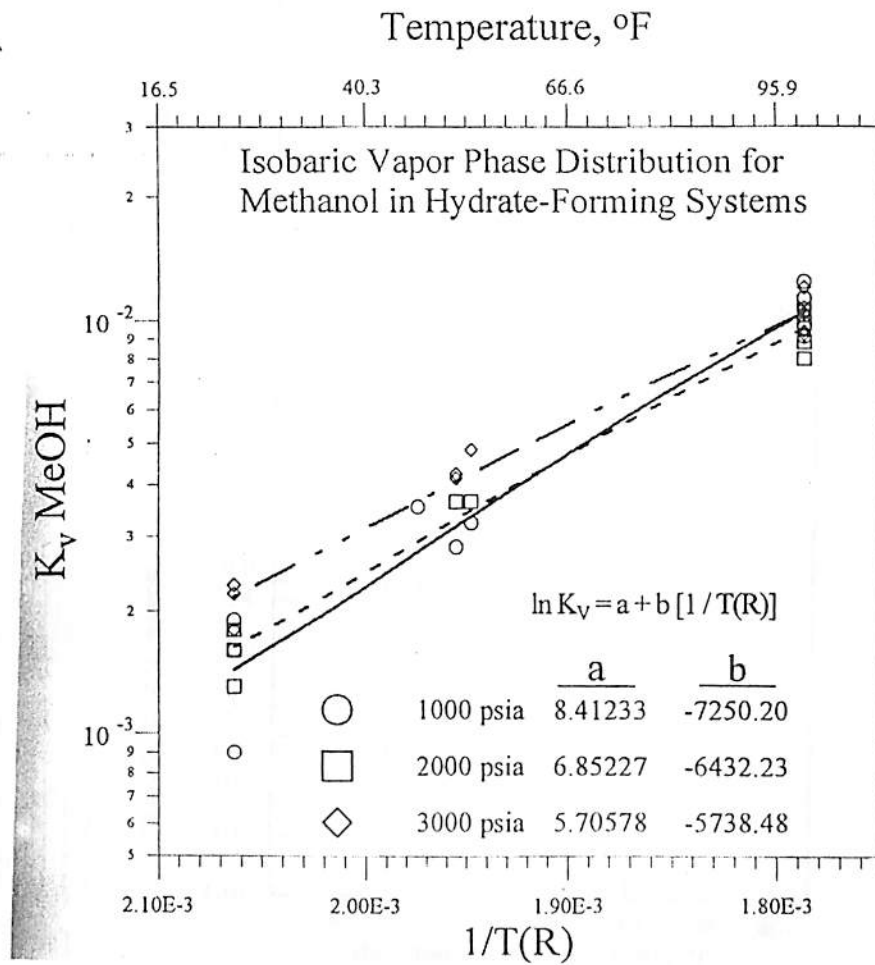
Figure 4.8 Loss of methanol to the vapor phase

Source: Clathtrate Hydrates of Natural Gases, Sloan(1998)
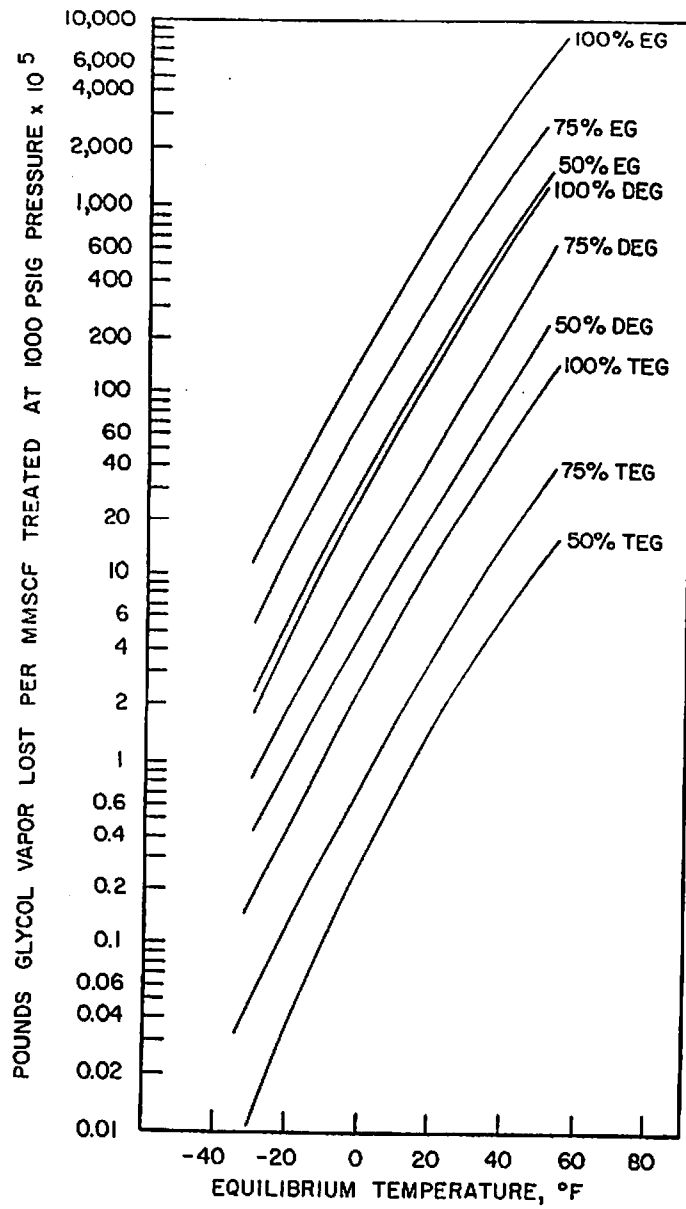
Figure 4.9 Loss of glycols to the vapor phase

Source: Clathrate Hydrates of Natural Gases, Sloan(1998)
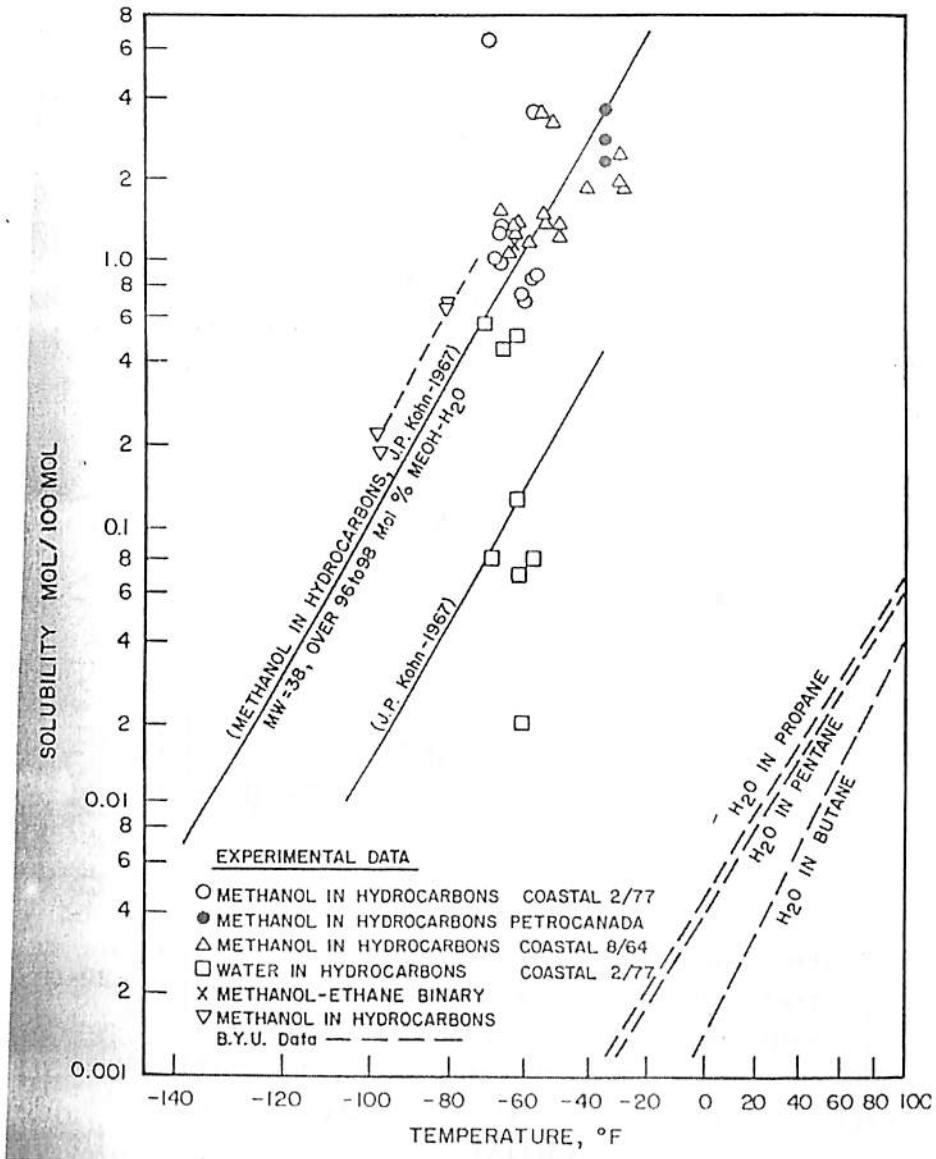
Figure 4.10 Solubility of methanol in liquid hydrocarbons

Source: Clathtrate Hydrates of Natural Gases, Sloan(1998)
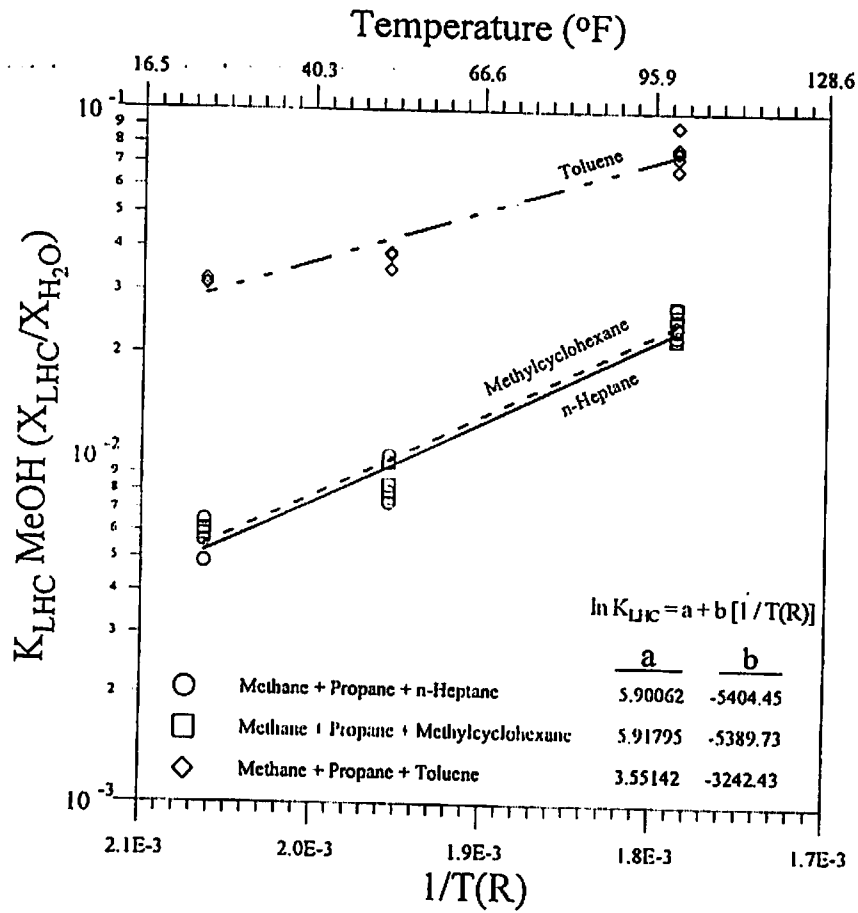
Figure 4.11 Pressure independent solubility of methanol in liquid hydrocarbons.

Source: Clathrate Hydrates of Natural Gases, Sloan(1998)
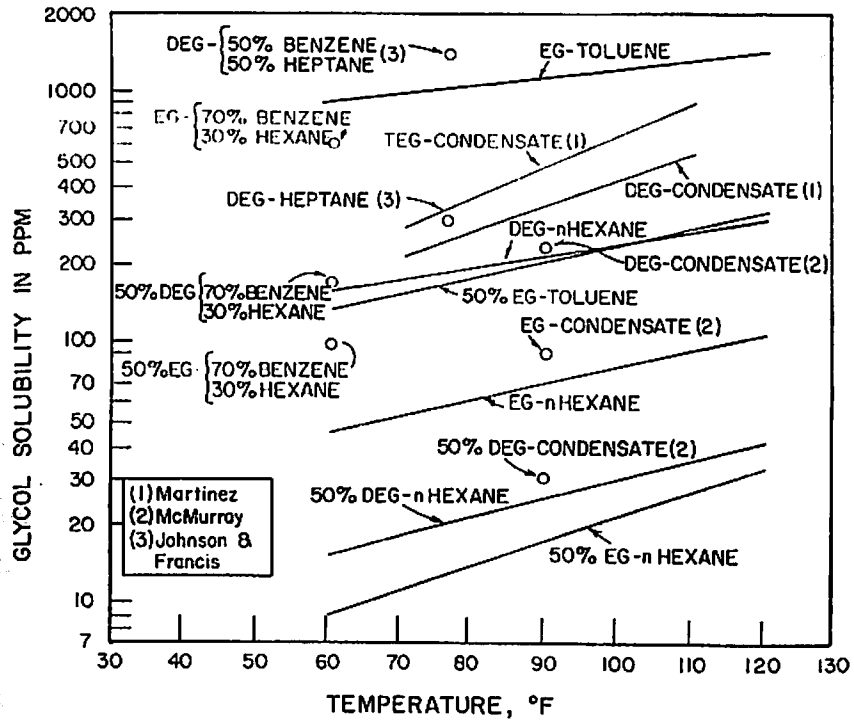
Figure 4.12 Solubility of glycols in liquid hydrocarbons

Source: Clathtrate Hydrates of Natural Gases, Sloan(1998)
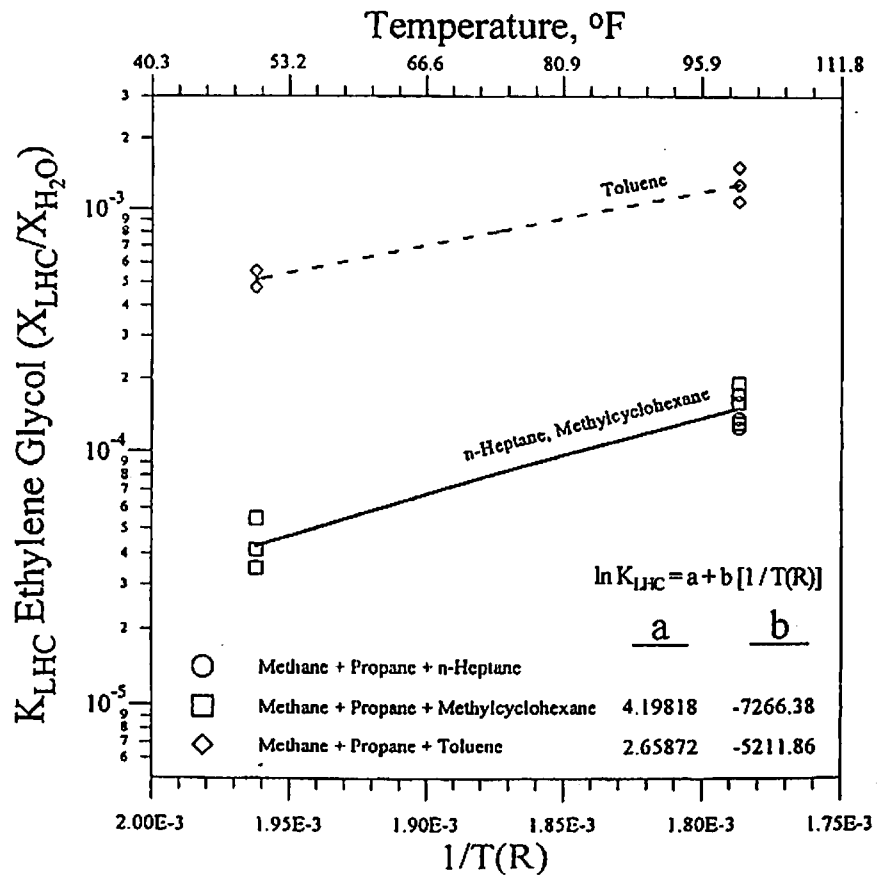
Figure 4.13 Pressure independent solubility of glycols in liquid
hydrocarbons

Source: Clathtrate Hydrates of Natural Gases, Sloan(1998)

4.5 Hydrate Control through Kinetic Inhibitors

Kinetic inhibition is a well-known technique in the oil industry for scale prevention but its use in hydrate inhibition is a relatively new technology. Sloan and coworkers distinguished its time dependence from the permanent time independence of the thermodynamic inhibition and were the first to use the term "kinetic inhibition". These chemicals can be effective at very low concentrations (< 1wt. %). They do not alter the thermodynamic conditions of hydrate formation. Kinetic inhibitors delay hydrate nucleation and subsequent crystal growth. These water-soluble compounds are inspired by antifreeze proteins (AFPs) secreted by some animal species to enable them to survive in sub-zero climates. Kinetic inhibitors are assumed to retard crystal growth by binding to the surface of hydrate particles in the early stages of nucleation and preventing the particle from reaching its critical size (the size at which particle growth becomes thermodynamically favourable). The duration of kinetic inhibition can be from several hours to days, which may exceed the residence time of fluids in process flowlines.

Kinetic inhibitor effects appear to be independent of the amount of water in a system, and since the water cut increases as a reservoir depletes, this gives them an advantage over thermodynamic inhibitors. However, shortcomings have been detected when the system presents more than 10 ^0C subcooling (defined as temperature of normal hydrate formation minus real operational temperature), and at extremely high pressures. After testing more than 750 combinations of different chemical inhibitors, Long et al (1994) found high molecular weight polyvinylpyrrolidone (PVP) to be a good hydrate inhibitor. In a similar study, involving the testing more than 1500 commercially available chemical combinations, three more chemical compounds with kinetic inhibition properties were found at the Colorado School of Mines. These products were poly(N-vinylcaprolactam) or PVCap, a terpolymer, Nvinylpyrrolidone/

N-vinylcaprolactam/N, Ndimethylmethacrylate, with the commercial acronym of VC-713 and a co-polymer of N-vinylpyrrolidone and Nvinylcaprolactam (VP/VC) made with different ratios of each constituent monomer. These kinetic inhibitors are illustrated in Figures 4.14-4.17.
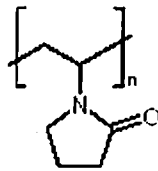
Figure 4.14 Unit structure of poly(N-vinylpyrrolidone)

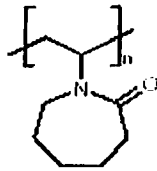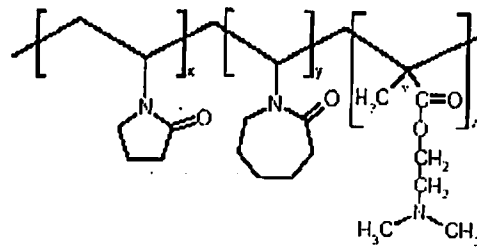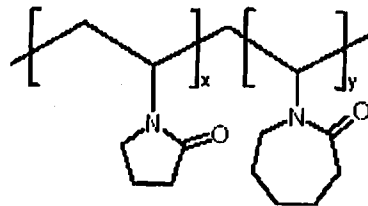*Source: Presentation at the SPE Production Operations Symposium held in Oklahoma City, Oklahoma, 26-28 March 2001.*

Figure 4.15 PVP,and Poly(N-vinylcaprolactam) PVCAP

Source: Presentation at the SPE Production Operations Symposium held in Oklahoma City, Oklahoma, 26-28 March 2001.

Figure 4.16 Polymer N-vinylcaprolactam-N-vinylpyrrolidone and
dimethylaminoethyl methacrylate Gaffix VC-713.

Source: Presentation at the SPE Production Operations Symposium held in
Oklahoma City, Oklahoma, 26-28 March 2001.

Figure 4.17 Poly(N-vinylpyrrolidone-co-N-vinylcaprolactam) VP/VC.

Source: Presentation at the SPE Production Operations Symposium held in
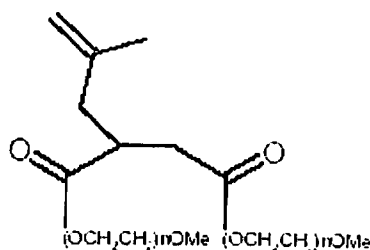Oklahoma City, Oklahoma, 26-28 March 2001.

2005

4.6 Anti-Agglomerants

These chemicals are polymers and surfactants, which are also added at low concentrations (<1wt.%). They allow hydrate formation, but work by preventing agglomeration of hydrates so that the hydrate crystals do not grow large enough to plug flowlines, but are transportable as a slurry[9]. Anti-agglomerants only work in the presence of both water and liquid hydrocarbon phases but the mechanism of inhibition is not well understood. For some classes of anti-agglomerants, the chemicals seem to act on the newly-formed hydrate nuclei as an emulsifying agent. Kelland *et al* (1995)[9], propose that emulsification is the mechanism, which prevents the hydrates from agglomerating. Thus, the anti-agglomerant effect may depend on the mixing process at the injection point and be enhanced by turbulence in the system. Increasing salinity or water cut (up to a maximum of 40 % water by volume) decreases the effect of antiagglomerants. Oil and condensate composition may also affect anti-agglomerants performance. However, anti-agglomerants do not appear to be adversely affected by extreme temperature and pressure conditions. The IFP (Institute Française du Petrole) and Shell are some of the pioneers in this technology. Figures 4.18-4.20 illustrate some of the first products tested by IFP.

Kelland *et al* (1995) developed a curve that shows the theoretical pressure-temperature limitations for use of hydrate inhibitors. In this curve, a safe pressure/temperature region is delineated for low-dosage inhibitors known at the time the curve was constructed. The diagram also includes predicted curves for theoretical future discoveries.
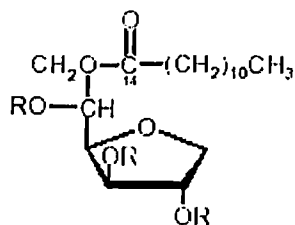
Figure 4.18. Ethoxylated sorbitan monolaurate [R=(CH2CH2O)nH].
Source: Presentation at the SPE Production Operations Symposium
held in Oklahoma City, Oklahoma, 26-28 March 2001.

Figure 4.19. Polymers of isobutylene succinate diester of
monomethylpolyethylene glycol. (monomer unit).
Source: Presentation at the SPE Production Operations Symposium
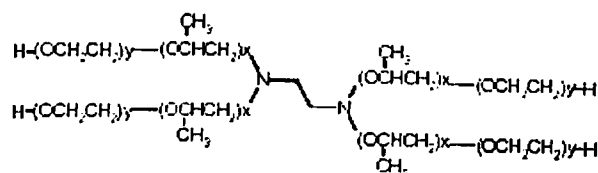*held in Oklahoma City, Oklahoma, 26-28 March 2001.*

Figure 4.20. Ethylene diamine-based block PO-EO copolymers.
Source: Presentation at the SPE Production Operations Symposium
held in Oklahoma City, Oklahoma, 26-28 March 2001.

71

4.7 Deployment of Low-Dosage Inhibitors

High operating, supply, and environmental costs associated with the use of methanol and glycol make them unattractive as hydrate inhibitors. Health, safety, environmental, and economic concerns have motivated the petroleum and gas industry to search for more feasible (or competitive) solutions such as low-dosage inhibitors. Even though low-dosage inhibitors appear to be a good replacement for thermodynamic inhibitors, only a few case studies of successful low-dosage inhibitor deployment have been published. There are more documented cases of kinetic inhibitor deployments than of anti-agglomerants, and even less has been written about optimized low-dosage inhibition programs incorporating both kinetic inhibitors and anti-agglomerants over the course of a reservoir life span. Industry does not go ahead with using a new hydrate inhibition method in a new processing facility unless it is very sure that it will work as intended.

In order to use a low-dosage inhibitor, careful consideration must be given to any potential effect that will compromise production operations, as well as the efficacy of any additional additives.

Successful deployment of low-dosage inhibitors in place of thermodynamic inhibitors have been reported in the UK sector of the Southern North Sea, the Gulf of Mexico in USA, Texas and South-western Wyoming, in the Gulf of Paria near Trinidad and in the South West of France whereas in, Canada and the Middle East, trials have not met with complete success. Successful deployment of low-dosage inhibitors depends on rigorous testing and good understanding of the field conditions.

The hope for low-dosage inhibitors has been that they would replace traditional thermodynamic inhibitors, but their action does not yet cover extreme conditions.

Reservoirs in environments with temperatures below 0oC would require antifreeze addition for controlling ice formation even if hydrate formation was not a threat. Under these conditions, extreme temperatures and pressures cause operators to use combined thermodynamic and low-dosage inhibitors. The topography of the pipeline also plays an important role in the performance of low-dosage inhibitors. In locations where the local residence time of the fluids is longer than the induction time of the low-dosage inhibitor used, gas hydrate plugging can occur. Gas pipelines represent a special case, because if the liquid phase is vaporized there is no solvent to carry the inhibitor and consequently, the inhibition effect could be lost. Shutdown conditions are different from normal operating conditions since the residence time of the fluids is extended and temperatures can drop. This is an important aspect to keep in mind when planning a hydrate inhibition strategy. For example, addition of glycol or methanol during a shut-down is a typical short-term solution. Restarting also represents abnormal operating conditions where velocity and pressure of the fluids can be greatly increased.

Since experimental conditions are quite different from real field conditions, scale-up criteria must be developed in order to obtain similar or correlated results. Lederhos and Sloan (1996) worked on the transferability of results between two small bench scale apparatus and a pilot scale flow loop, evaluating the performance of kinetic inhibitors in terms of subcooling. However, few publications deal with the issue of scale-up. Although operating conditions can be simulated in the lab, unnaturally clean conditions and the scale of the tests do not permit direct application of result to the field.

Philips and Grainger give a useful guide for studying the application of low-dosage inhibitors (in this case, kinetic inhibitors) as a replacement for conventional thermodynamic techniques. This study is an aid, which, if properly used, will give the

operator a deep understanding of the field conditions, which can be. It is based on a detailed preliminary survey. Philips and Grainger propose several questions as a basis to such a survey.

A survey can be formulated to collect the most accurate information describing the system conditions. Once these conditions are well understood, lab tests can be performed. The best low-dosage inhibitor for the system conditions is selected, and a complete experimental design will guarantee its field performance with a good degree of confidence.

CHAPTER-5
FUTURE RESEARCH

5 Future Research

1. There is still a long way to go in gas hydrates prevention research. The main objective is to develop hydrate inhibitors that work under a large range of conditions and at very low concentrations. These new techniques would ideally be good enough to completely replace thermodynamic inhibition, since they are currently deployed commercially using thermodynamic inhibitors as carrier chemicals. In order to contribute to the development of this technique, we propose a direction for future research.

2. Molecular level mechanisms of hydrate inhibition with low-dosage inhibitors are still not understood. Work in this direction requires the development of new experimental techniques for probing and recording microscopic interactions through time.

3. The use of techniques borrowed from biotechnology may provide insight into the gas hydrate problem. Hydrate inhibiting chemicals inspired by nature, and the use of biological systems to study the kinetics of hydrate formation are two key examples, and further work in this area is encouraged.

4. Development of new low-dosage inhibitors, or combinations of chemicals able to work in more extreme conditions (higher pressures, lower temperatures, higher water cuts), having both kinetic and anti-agglomerant properties and compatible with other additives.

5. Development of relationships between required lowdosage inhibitor types and amounts, and system temperature, pressure, and chemical conditions (including volume of water and composition of hydrocarbon constituents and additives).

6 Conclusions

1. Hydrate formation is a very expensive problem faced by the oil and gas industry, which must be solved in an economically and environmentally appropriate manner. Low-dosage inhibitors appear to be part of this solution, but shortcomings persist.

2. Successful deployment of low-dosage inhibitors depends on an appropriate selection of inhibitors and a complete understanding of the system. Because each processing facility or pipeline is unique (in terms of stream chemistry and operating conditions), and hydrate formation theory is too vague to allow accurate prediction of inhibitor action, well-designed lab tests must be performed. If a product trial were attempted without experimental studies, it would be difficult to understand the cause of its success or failure.

3. Even when low-dosage inhibitors appear to be the best option for the prevention of gas hydrates, there are few cases of field trials or successful replacement of thermodynamic inhibitors, which continue to be the industry mainstay.

4. In many cases, especially for applications in severe environments, commercial deployment of low-dosage inhibitors is being offered to reduce the consumption of thermodynamic inhibitors rather than to replace them. Low-dosage inhibition must be developed to work under more extreme conditions of pressure and temperatures if more extreme conditions of pressure and temperatures.

References

1. Hammerschmidt, E. G.: "Formation of Gas Hydrates in Natural Gas Transmission Lines," *Ind. & Eng. Chem.* (1934) v. 26, 851.

2. Sloan, E. D., Jr.: *Clathtrate Hydrates of Natural Gases*, second edition, Marcel Dekker, Inc., New York, USA (1998).

3. Presentation at the SPE Production Operations Symposium held in Oklahoma City, Oklahoma, 26-28 March 2001.

4. Makogon, Y. F. et al.: "Gas Hydrate Formation and Dissociation with Thermodynamic and Kinetic Inhibitors,"(1999)

5. Panchalingam, V. and Sloan, E.D.: "Hydrate Kinetic Inhibition Chemicals," (1996)

6. J.A. Ripmeester, J.S. Tse, C.I Ratcliff, and B.M. Powell, Nature, (1987)

7. S. Subramanian, R. Kini, S.F. Dec, E.D. Sloan, (2000).

8. M.D. Jager, C.J. Peters, E.D. Sloan,(2000).

9. Gudmundsson, J.S., Mork, M. and Graff, O.F., Hydrate non-pipeline technology, (2002)

10. Andersson.V, Flow properties of natural gas hydrate slurries (1999)

List of Tables

List of Figures